High carnallite-bearing material for thermochemical energy storage: Thermophysical characterization

Andrea Gutierrez[1], Svetlana Ushak[2], Marc Linder[1]

[1]German Aerospace Center – DLR e. V., Institute of Engineering Thermodynamics,

Pfaffenwaldring 38, 70569 Stuttgart, Germany

[2]Department of Chemical Engineering and Mineral Processing and Center for Advanced

Study of Lithium and Industrial Minerals (CELiMIN), Universidad de Antofagasta, Campus

Coloso, Av. Universidad de Antofagasta 02800, Antofagasta, Chile

Corresponding author: andrea.gutierrezrojas@dlr.de (A. Gutierrez)

ABSTRACT. Thermochemical energy storage has a high material-related energy density and

low energy losses over time compared to sensible and latent energy storage. Considering

economic and ecological aspects, there is a great opportunity in using low cost or even waste

materials from the mining industry, as thermochemical energy storage medium. In this study,

a systematic analysis of a high carnallite-bearing material, comparable to the natural waste,

for thermochemical energy storage was performed. The material displays gradual

decomposition and poor reversibility of hydration reaction at temperatures above 150°C.

However, the reversibility is significantly higher and the decomposition is slower between

21   100°C and 150°C under p_{H2O}=25 kPa. The reversible behavior of hydration reaction of

22   carnallite, between 100°C and 150°C, is stable for 15 cycles when the material is exposed at

23   150°C for short periods of time (t < 20 min). Following this path, any potential application of

24   this material is definitely limited to low temperature thermal storage or thermal upgrade.

25   Taking the low material cost into account one of the potential applications of this material

26   could be in the context of long-term heat storage. For this purpose, the temperatures of

27   dehydration can be below 150°C and the temperatures of rehydration close to 40°C.


28   INTRODUCTION

29   Thermal energy storage (TES) has been identified as one of the key technologies for a

30   sustainable and continuous supply of renewable energy. Thermal energy can be stored

31   whenever the source is available, for example during the day or in summer. The heat can then

32   be released when it is required, for example during the night or in winter.

33   There are three well-known mechanisms for storing thermal energy that are briefly described

34   below. For each of these concepts, there is a wide variety of materials applied as medium of

35   storage, such as paraffines, fatty acids, rocks, water, nitrate salts and salt hydrates among

36   others.[1,2] The inorganic salts addressed in this paper could be applied as storage materials for

37   all three concepts. Regarding this, several studies have been published showing a high

38   potential of use of by-products or wastes from inorganic mining as TES materials.[3-6] By

39   utilizing currently unexploited inorganic wastes as a storage material, critical aspects like the

40   energy burden of storage materials, economic aspects as well as ecological aspects, e.g. due

41   to mining, can be tackled at the same time. Recent approaches and results concerning thermal

42   energy storage based on inorganic waste materials can be found in the given references:

43   •   Sensible heat storage (SHS): the amount of energy stored/released while the

44   temperature of the inorganic salt is increased/decreased,[1,7]

45   •   Latent heat storage (LHS): the amount of energy stored/released when the inorganic

46   salt changes phase,[2,7]

47   •   Thermochemical storage: the amount of energy stored/released when a reversible

48   reaction takes place, e.g. hydration/dehydration of inorganic salts.

49 The main advantages of thermochemical storage materials (TCM) compared to sensible

50 (0.033-0.4 GJ/m^3) and latent heat storage (0.15-0.37 GJ/m^3) [1,8], are their high material-related

51 energy densities (0.92 – 3.56 GJ/m^3) [9] and low energy losses over time.[1,11,12] Additionally,

52 TCM exhibit a wide versatility of applications: one example is heat transformation, in which

53 thermal energy (forward reaction) can be stored at low temperatures and released at higher

54 temperatures (reversible reaction) by changing the pressure of the reaction system. [12-15]

55 However, as this mechanism involves a chemical reaction, some additional challenges have

56 to be faced, e.g. the complexity of components and especially material-related aspects like

57 cycling stability. [15,16] A typical gas-solid reaction system using salt hydrates is shown in Eq.

58 1. (Modified from [17])

$$MX \cdot nH_2O_{(s)} + \Delta_R H \leftrightarrow MX \cdot mH_2O_{(s)} + (n - m)H_2O_{(g)}, \qquad Eq. 1$$
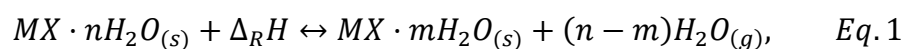
59 In this reaction MX·nH$_2$O$_{(s)}$ would be a salt hydrate which consists of MX·mH$_2$O$_{(s)}$ and (n-m)

60 mol of reactive water vapor. In order to deploy these technologies successfully, it is important

61 that they satisfy specific technical and economic requirements. Considering economic and

62 ecological aspects, there is a great opportunity in using low cost or even waste materials from

63 the mining industry. In doing so, the accumulation of wastes in mining sites can be also

64 reduced and potential long-term, harmful environmental impacts can be avoided. Several salt

65 hydrates are currently obtained as by-products or wastes from the mining industry, which are

66 natural material already available in the mining sites. These materials correspond mainly to

67 double salts such as carnallite, bischofite, kainite, astrakanite, darapskite and schoenite. They

68 contain from two to six mol water of crystallization per mol of anhydrous salt and are

69 therefore theoretically suitable for thermochemical storage with water vapor as a gaseous

70 reactant. The most critical point for a potential application of these salts is the reversible

71 reaction of hydration/dehydration. Gutierrez et al. 2017 have already studied the thermal

72 stability of three of these materials: potassium carnallite, lithium carnallite and astrakanite.

73 Results showed that potassium carnallite and astrakanite could have potential as

74 thermochemical storage materials, based only on their studies of thermal stability below

75 350°C.[6]

76 In this study, a systematic analysis of a high potassium carnallite-bearing material as

77 thermochemical energy storage medium was performed. In order to minimize the influence of

78 low-bearing impurities contained in the natural potassium carnallite, such as calcium sulfate

79 dihydrate, lithium chloride monohydrate among others,[18,19] the experimental study was

80 performed with a synthetic material. The reversibility of reaction was studied and the limiting

81 conditions of operation were evaluated, in order to investigate it suitability as a TCM.

82 Finally, based on its thermophysical properties some potential applications were discussed.

83 EXPERIMENTAL METHOD

84 Material

85 The compounds used to prepare the synthetic material were KCl (potassium chloride,

86 anhydrous powder, 99.5%, Merck) and $MgCl_2 \cdot 6H_2O$ (Magnesium chloride hexahydrate,

87 hygroscopic crystals, 99%, Merck). The sample was prepared by crystallization from ternary

88   equilibrium solution KCl-MgCl$_2$-H$_2$O at 35 °C. The precipitated crystals were separate from

89   the stock solution by vacuum filtration.

90   Chemical and Morphological characterization

91   Chemical analyses of the synthetic material were performed in order to calculate its chemical

92   composition. Potassium and magnesium concentrations were determined by atomic

93   absorption spectrometry. Chloride was determined by volumetric titration with AgNO$_3$ and

94   moisture was determined by drying until constant weight at 40 °C.

95   The mineral composition and morphology of crystals were analyzed using X-ray diffraction

96   (XRD) and scanning electron microscopy (SEM). Patterns of XRD (Bruker AXS - D8

97   Discover Bruker GADDS with a VANTEC-2000 detector) were recorded on a diffractometer

98   (using CuKα radiation) operating at 45kV/0.650 mA. A scanning rate of 0.5°/s was applied to

99   record the patterns in the 2θ angle range from 15° to 60°. XRD analyses for fresh sample of

100   carnallite and products after 5 cycles of hydration and dehydration were carried out. The

101   morphology and particle size of the crystals were examined by SEM (Zeiss ULTRA Plus). To

102   perform this experiment, a fresh sample of material was dehydrated overnight in a furnace at

103   120 °C surrounded by air and cooled in a desiccator to ambient temperature.

104   Thermal properties

105   Thermogravimetric –mass spectroscopy (TG-MS)

106   The thermal decomposition or reaction steps of the material were recorded by

107   Thermogravimetric analysis (NETZSCH STA 449 C Jupiter). A thermogravimetric sample

108   carrier with a thermocouple type S and an accuracy of ± 1 K was used. The accuracy of the

109   balance was ± 0.1 μg. The measurements were performed from room temperature (25 °C) to

110   1100 °C performing dynamic experiments with a heating rate of 5K/min using nitrogen as

111   protective gas with a volumetric flow of 50N-mL/min. The atmosphere surrounding the

112   sample was kept inert using 100 N-mL/min of nitrogen flow. In order to analyze the

113   generated gases, a Mass spectrometer (NETZSCH QMS 403 C Aëolos) was coupled to the

114   TG analyzer. Sample sizes of about ~50mg were measured in open Al_2O_3 crucibles.

115   STA –MHG reversibility of reactions

116   The reversibility of reaction and potential operating conditions were studied using a

117   Simultaneous thermal analyzer (NETZSCH STA-449 F3 Jupiter, see Figure 1). The set-up

118   was equipped with a Modular Humidity Generator (ProUmid MHG-32). A differential

119   scanning calorimetric and thermogravimetric (DSC-TG) sample holder with a thermocouple

120   Type P and an accuracy of ± 1 K was used. The accuracy of the balance was ± 0.1 µg.

121   Nitrogen was used as protective and purges gas with a volume flow for both of 20N-mL/min.

122   The atmosphere surrounding the sample was kept inert using 100 N-mL/min of nitrogen flow

123   and water vapor. Either pure nitrogen was used or a mix of nitrogen and water vapor. Liquid

124   nitrogen was used to support the controlled cooling process. Partial vapor pressures of 15 kPa

125   (15.9% RH), 25 kPa (30% RH) or 30 kPa (38% RH) were set as it is shown in Figure 2

126   named Experiment 1. According to literature the critical relative humidity (CRH) of

127   potassium carnallite (the main component of the synthetic material) is within the range of 50

128   – 55% at 30 °C.[20] However, the phase diagram of the $KCl \cdot MgCl_2$ (anhydrous compound

129   from potassium carnallite) in equilibrium with water is not available. This means that there is

130   no evidence that accurately shows how the CRH will vary with temperature. Under these

131   circumstances the maximum partial water vapor pressure was set to 30 kPa (38% RH).

132   Sample sizes of about ~15 mg were measured in open platinum crucibles (85 µL).
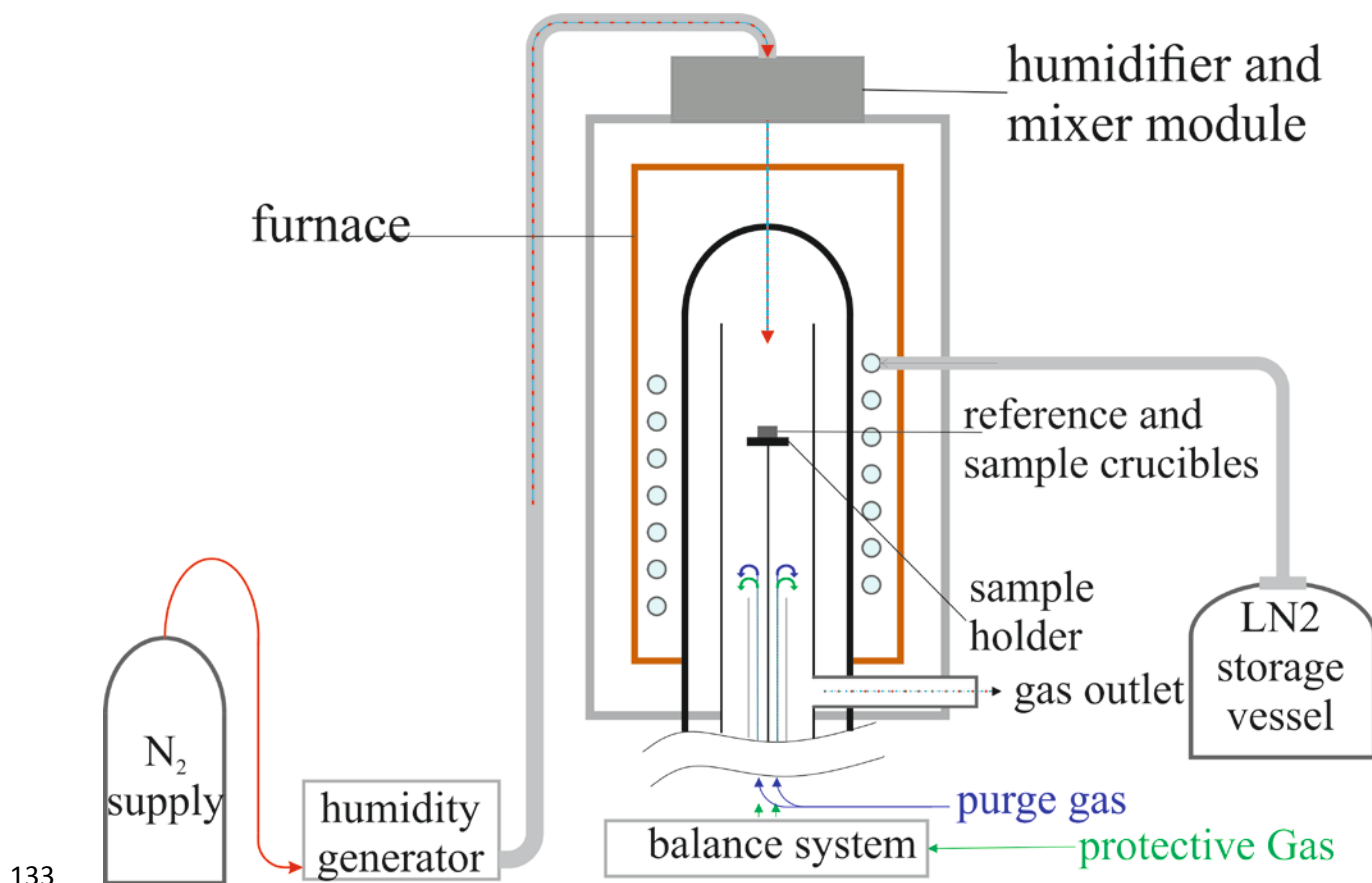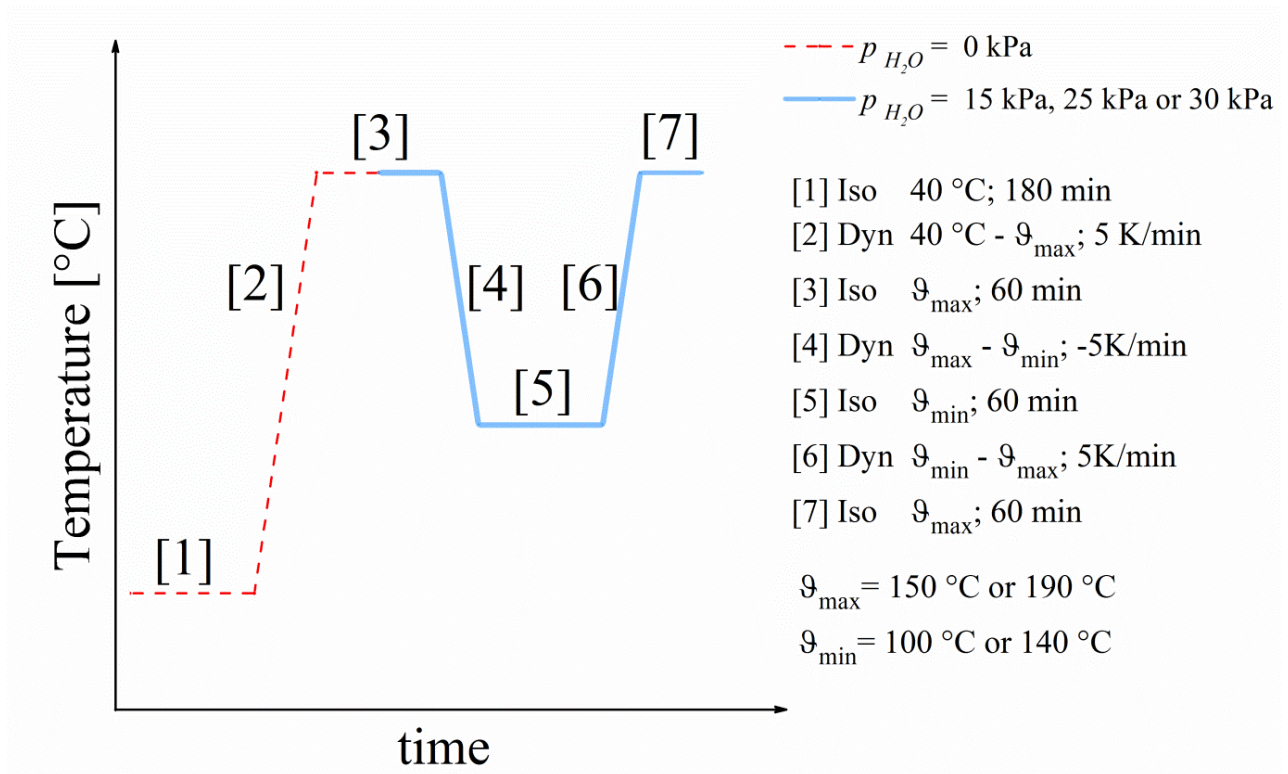
Figure 1 Schematic diagram of the simultaneous thermal analyzer (STA).

Dynamic experiments were carried out with heating/cooling rates of 5 K/min. The temperatures of hydration were set to a minimum of 100°C, due to the hygroscopic/deliquescent behavior of samples previously mentioned.

Figure 2 Experiment 1: Temperature and humidity program to study the reversibility of reactions.

RESULTS AND DISCUSSIONS

Chemical and morphological characterization

Considering the composition of the product on dry basis, the results of chemical analyses for ions and water of crystallization (in wt. %) of the synthesized material are shown in Table 1.

Table 1 Synthetic material composition (wt. %)

Element	Mg^{+2}	K^+	Cl^-	H_2O
Composition	9.28	11.76	37.73	41.22

Figure 3 shows the XRD diffractogram of the synthetic material (fresh sample) where two phases were identified, potassium carnallite (hereinafter called "carnallite"; KCl·MgCl$_2$·6H$_2$O) and magnesium chloride hexahydrate (MgCl$_2$·6H$_2$O).

149
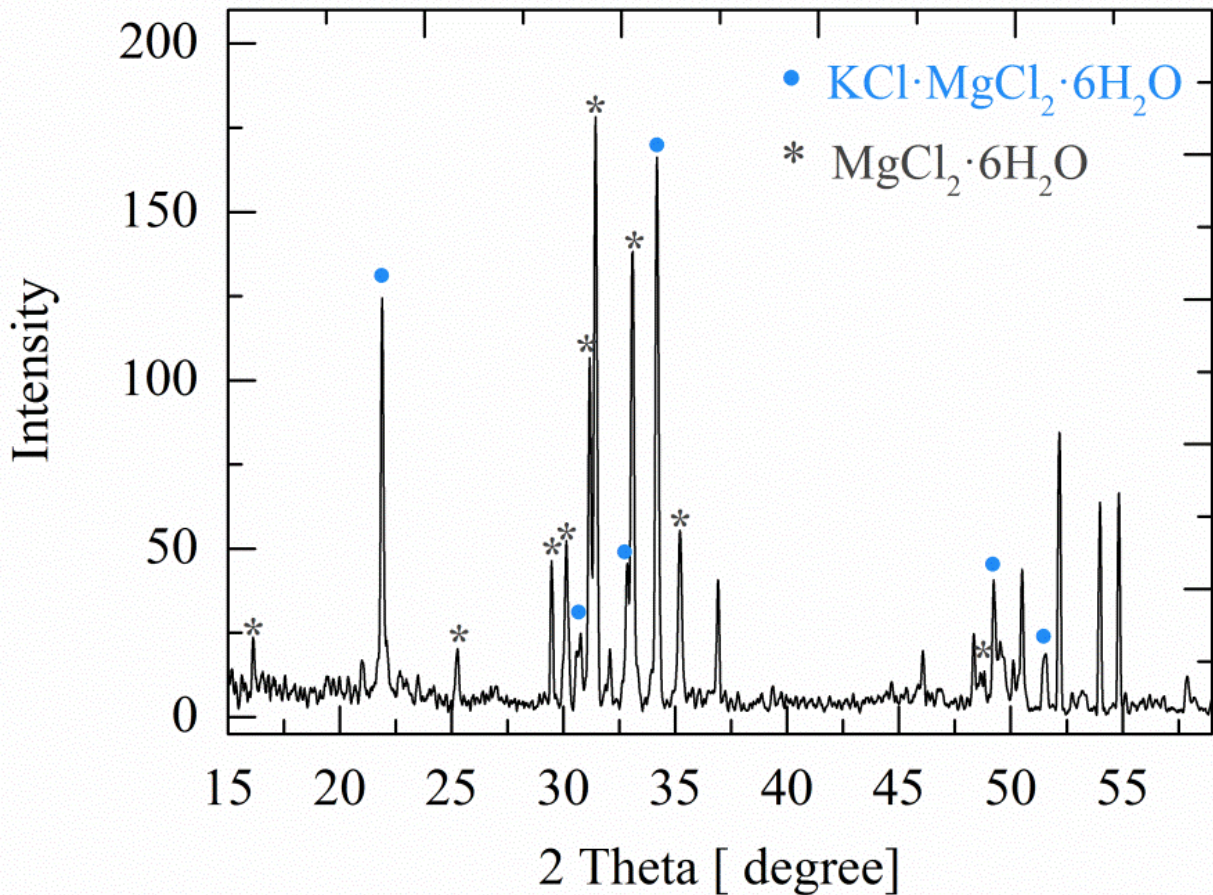
Figure 3 XRD diffractogram of fresh sample used for this study.

151 Taking into account the phases identified by XRD and the chemical analysis results, the

152 calculation of the mineralization was carried out. The weight percentage (wt. %) composition

153 of the sample is shown in Figure 4, where it can be seen that the content of carnallite is 76.53

154 wt.%, magnesium chloride hexahydrate 15.05 wt.% and the content of stock solution is 8.43

155 wt. %, the latter was presumable soaked into the sample crystals. The amount of carnallite

156 contained in the material it is in agreement with the natural waste obtained from Salar de

157 Atacama in Chile, that contains from 60 wt. % to 73.77 wt. % of $KCl \cdot MgCl_2 \cdot 6H_2O$ plus

158 impurities such as NaCl, KCl and $CaSO_4$.[18,19]. This waste precipitates in the solar evaporation

159 ponds during the processes to obtain lithium carbonate and potassium chloride. Additionally,

160 if the water contained in the stock solution of the synthetic material evaporates completely

161 then magnesium chloride hexahydrate would precipitate. If this is the case, the new

162   theoretical composition of the synthetic material would be carnallite 83.6 wt. % and

163   magnesium chloride hexahydrate 16.4 wt.%.

$$KCl \cdot MgCl_2 \cdot 6H_2O$$
$$76.53\%$$

$$MgCl_2 \cdot 6H_2O$$
$$15.05\%$$

Stock solution
8.43%
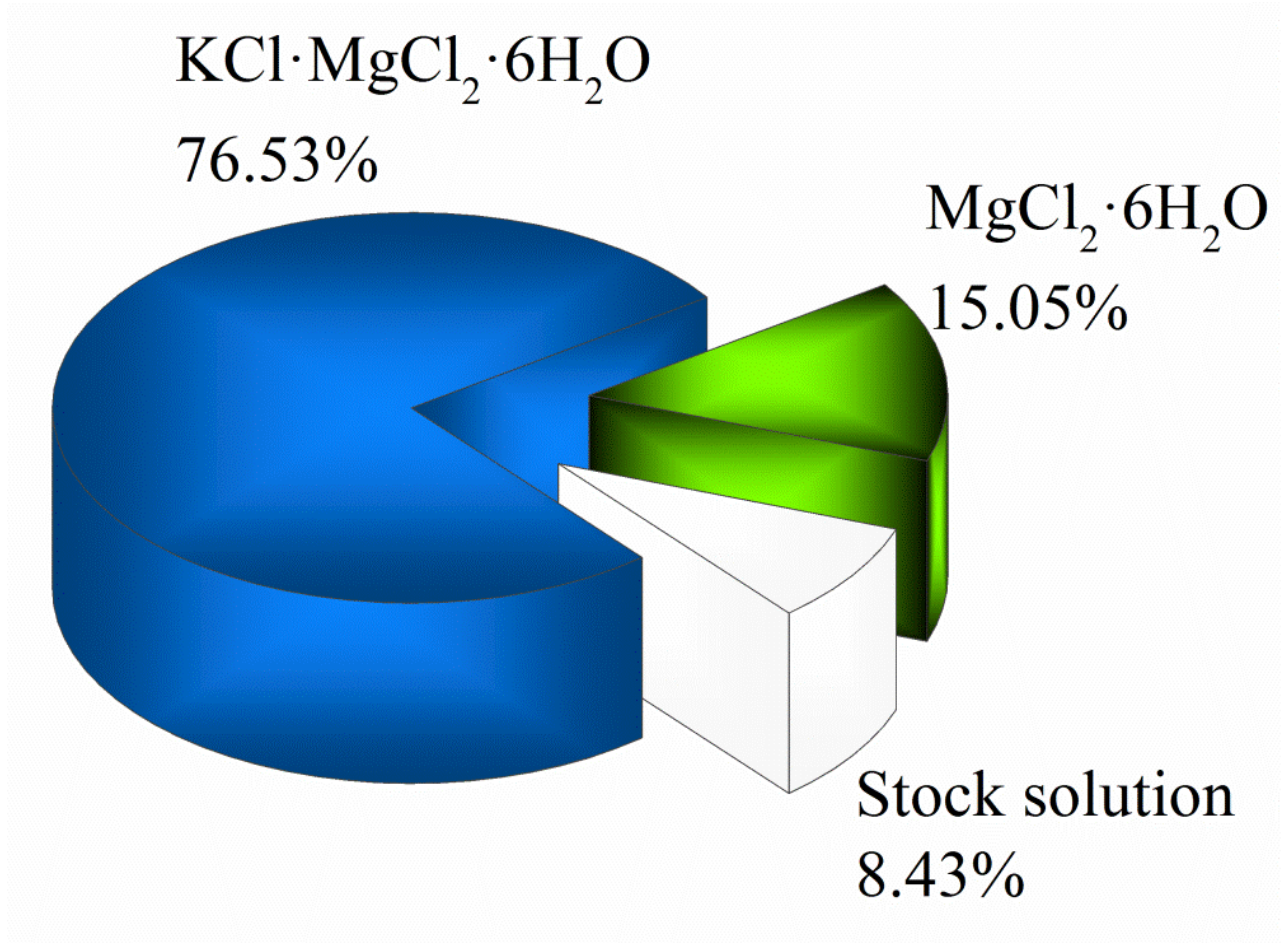
164

165   Figure 4 Weight composition of fresh synthetic material

166   Using SEM, the morphology of the dehydrated product obtained from the synthetic material

167   was determined (Figure 5). It can be seen that the dried crystals have an undefined and

168   irregular form, presenting a porous surface and also some surface cracks obtained as a results

169   of the dehydration of carnallite and magnesium chloride hexahydrate in atmosphere of air.

(a)   (b)
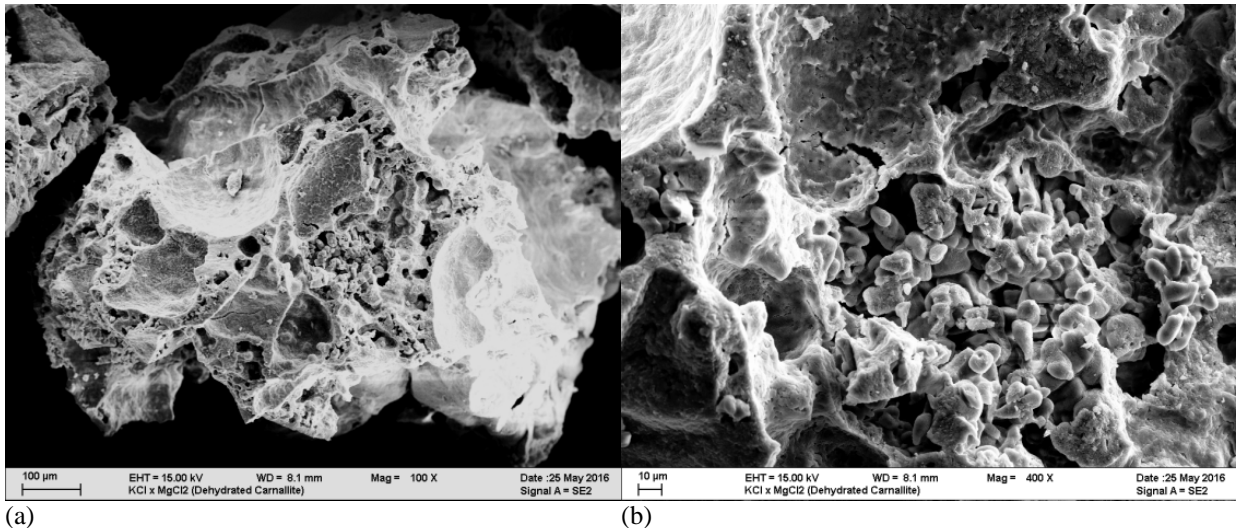
170   Figure 5 SEM images of dehydrated material at (a) x100 and (b) x400.

171   Thermal Properties

172   Thermogravimetric – mass spectroscopy (TG-MS)

173   The investigation of the reaction steps of dehydration, resulting from the TG experiments

174   (Figure 6), shows a weight loss in two steps below 260 °C (green curve). As the sample is

175   composed by two different salt hydrates it is not possible to determine, only with the TG

176   results, if both salts are reacting and neither what the ratio of dehydration reaction between

177   them is.

178   However, useful information regarding the decomposition of the synthetic material can be

179   obtained from the MS results. The first step of mass loss was identified by MS as mainly

180   water vapor (blue curve), with a small amount of HCl close to 180°C (orange curve). The

181   second step corresponds to a partial mass loss of 19.00 wt. % (5.00 wt. % + 14.00 wt.%, up to

182   ~260 °C), which was identified by MS as water vapor and HCl. In contrast to the first step,

183   the second step presents a significant increase of HCl release starting at 204 °C. This step of

184   dehydration takes place from 167 °C to 260 °C. Some authors report that a lower hydrate of

185   magnesium chloride hexahydrate as well as of carnallite release HCl as a results of partial

186   hydrolysis starting at 120°C and 200°C respectively.[22-24] Thus the mass losses showed in

187   Figure 6 correspond to the dehydration reaction of both salt hydrates present in the synthetic

188   material. However, the mass balance based on the stoichiometric calculation indicates that in

189   case of complete dehydration reaction of both materials plus the evaporation of water present

190   in the stock solution, the mass loss should be 46.2 wt. %. As the mass loss at 260°C is only

191   42.5 wt. % it can be assumed that the water available in the fresh material is not completely

192   released. This could be due to partial dehydration of both salt hydrates and/or partial

193   evaporation of the water contained in the stock solution.
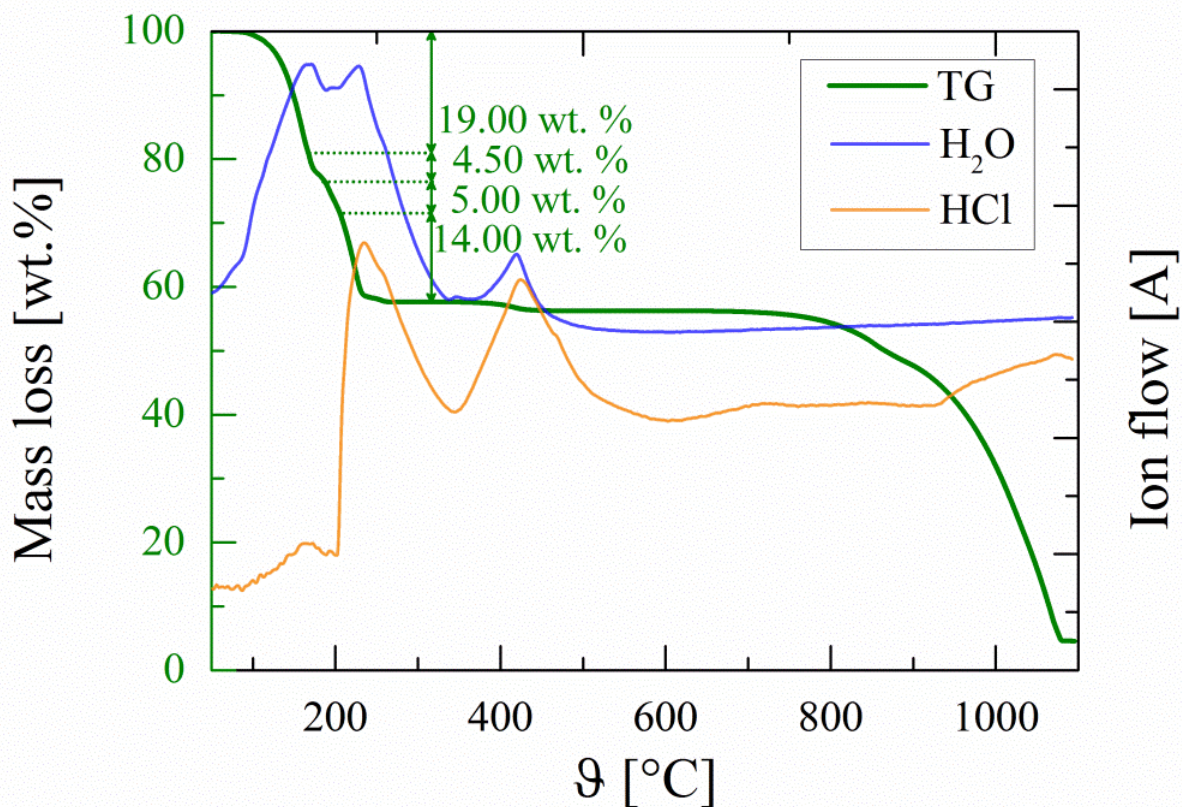

194

195   Figure 6 Thermal decomposition of carnallite, TG-MS curves. Heating rate of 5 K/min

196   Due to the hazardousness of HCl and the irreversibility of this reaction in humid

197   atmospheres, the temperature range of this study was limited to temperatures below 200 °C to

198   take potential applications into consideration.

Reversibility of reactions

199

200 The experiment 1 to evaluate the reversibility of reactions followed the temperature and

201 humidity program shown in Figure 2. The first results obtained are summarized in Figure 7

202 (a) rehydration reaction (segments 3-5 of experiment 1) and Figure 7 (b) (segments 5-7 of

203 experiment 1). To carry out the calculations of level of hydration it was assumed that only

204 potassium carnallite was reacting. This is due to the thermophysical properties of magnesium

205 chloride hexahydrate such as melting point at 117°C, and solidification point at 75°C,[3]

206 besides of magnesium chloride in equilibrium with water at temperatures above 100°C and

207 RH above 15% is either magnesium chloride hexahydrate or is in liquid state. [17] Thus, the

208 increase of mass, according to our assumption, corresponds only to the rehydration of

209 $KCl \cdot MgCl_2$, and the level of hydration and dehydration are shown in Figure 7. It can be seen

210 that the three experiments present two steps of hydration (Figure 7 (a)) as well as two steps of

211 dehydration (Figure 7 (b)) and they are clearly identifiable. This two-step

212 dehydration/hydration behavior is also similar to that reported by Molenda et al. 2013 for

213 $CaCl_2 \cdot 2H_2O$.[21] Even though the operating conditions were quite different, the two-steps

214 hydration behavior remains constant under different water vapor partial pressures. However,

215 the two-steps dehydration was slightly different at lower water vapor partial pressures. In this

216 study, it is observed that the three samples shown complete hydration/dehydration reactions,

217 only the sample under 30kPa shows slower dehydration in the second step. Based on this the

218 intermediate value of 25 kPa was chosen to continue with further experiments.

219
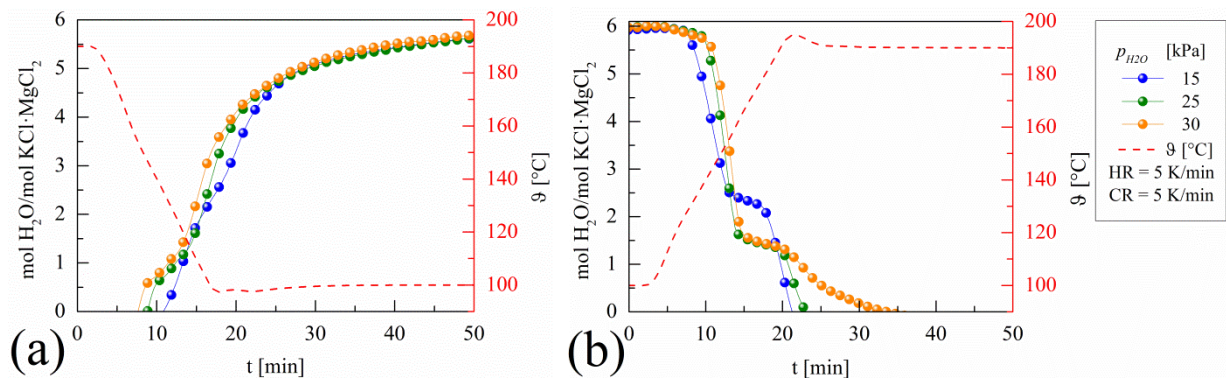
Figure 7 Level of (a) hydration and (b) dehydration of anhydrous carnallite

Figure 8 is a closer look at the level of hydration of experiment 1 using 25 kPa of partial

vapor pressure in terms of mass percentage. Additionally, the first dehydration step (dynamic

phase) performed under dry atmosphere of nitrogen is shown. According to the results

obtained from experiment 1, a combination of high temperature and humid atmosphere leads

to a continuous mass loss of sample (see the arrow starting at two hours) that might be due to

the formation of gaseous HCl from magnesium chloride hexahydrate, or a lower hydrate from

this salt. With decreasing temperature (dynamic phase), the mass of the sample starts to

increase due to the rehydration of the anhydrous phase, that as it was mentioned before would

correspond only to the hydration of $KCl \cdot MgCl_2$.
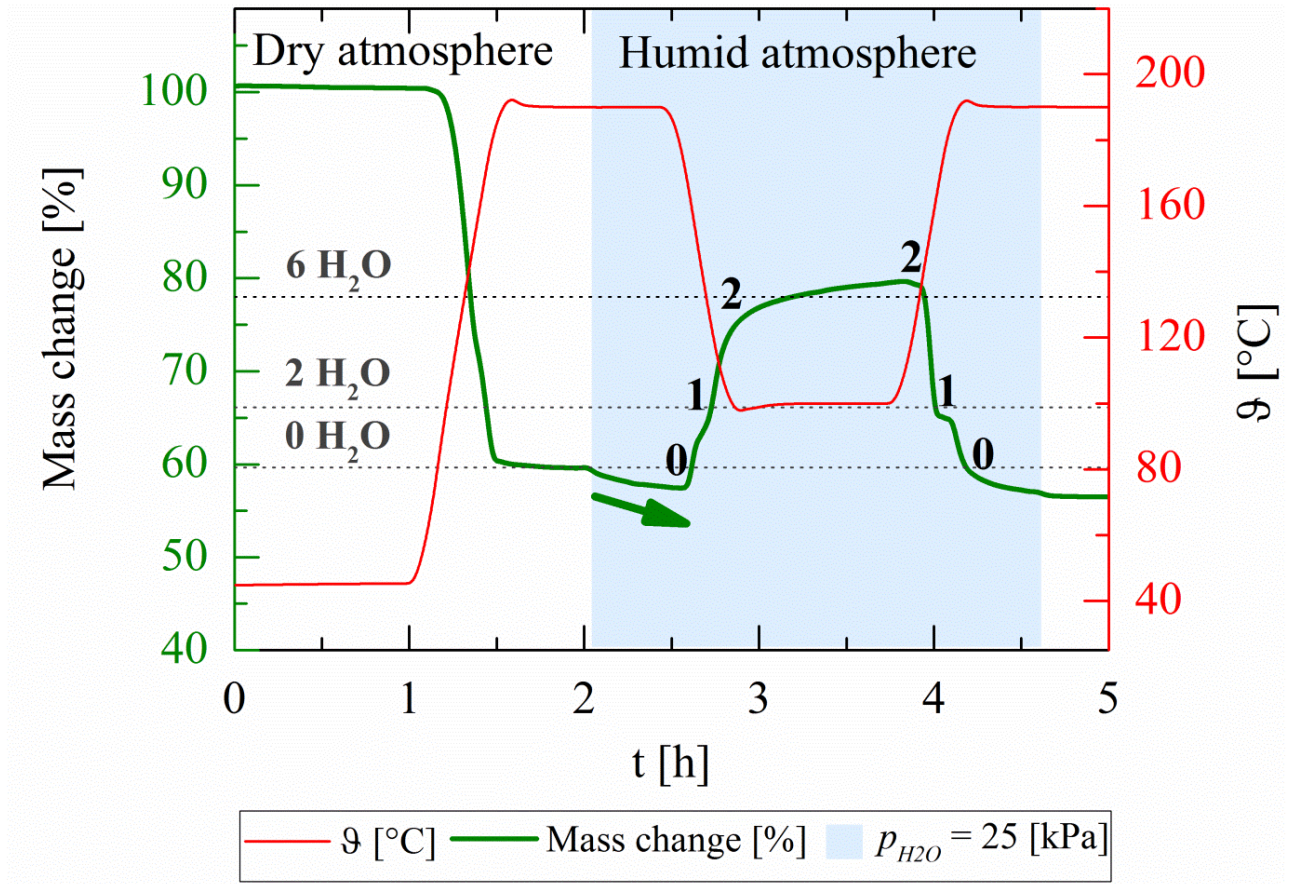
Figure 8 Percentage mass changes due to dehydration-hydration reactions of potassium carnallite and sub-products (p_{H2O}= 25 kPa).

The temperatures of hydration/dehydration depend on the gas pressure (p_{H2O}) according to the van't Hoff equation (Eq. 2).

$$ln\left(\frac{p_{H_2O}}{p^+}\right) = \frac{\Delta_R S^\theta}{Rv} - \frac{\Delta_R H^\theta}{RvT} \qquad Eq.\,2$$

Where, p_{H2O} is the water vapor partial pressure (kPa), p^+ the reference pressure (100 kPa), $\Delta_R S^\theta$ (J/(mol K)) and $\Delta_R H^\theta$ (kJ/(mol K)) the standard entropy and enthalpy of reaction, respectively. **R** is the universal gas constant (8.314 J/(mol K)), v the stoichiometric factor for each reaction and T the temperature (K). The estimated values of entropy of reactions from 150±5 J/(mol K) reported by Richter et al.[15] were used. The enthalpy of reaction was calculated based on literature data available for the standard enthalpy of formation ($\Delta_f H^\theta$).

241   Replacing all these values in Eq. 2, the van't Hoff diagram for carnallite and $MgCl_2 \cdot 6H_2O$

242   was built and is shown in Figure 9. It can be seen that the experimental results shown in

243   Figure 7 are in agreement with the theoretical equilibrium temperatures of carnallite. The

244   empty markers correspond to the dehydration temperatures of reactions from Figure 7, and

245   the filled markers corresponds to the hydration temperatures of reaction from the same figure.

246   This preliminary confirms that the measured mass change during the reversible reaction could

247   not be related to the whole sample mass but only to the content of carnallite, (76.53 wt. %) of

248   fresh material, which corresponds to the 'active' material of the sample. However, there are

249   still two issues to solve. The first is that the hydration curve (mass increase at low

250   temperature) does not reach the equilibrium, this can be deduced from the continues increase

251   of mass at low isothermal temperature. And second, the equilibrium temperature of $MgCl_2$

252   from 4-2 is very close to the equilibrium temperature of $KCl \cdot MgCl_2$ from 2-0. This could

253   explain why the mass is continuously increasing without reaching the equilibrium, because

254   the $MgCl_2$ must still be active. Despite of it, carnallite seems to be promising because the

255   reaction is detected close to the theoretical equilibrium and, measured with relatively fast

256   heating and cooling rates of 5 K/min, only a small hysteresis can be observed. However,

257   since a combination of water vapor and high temperature leads to a complete or partial

258   hydrolysis reaction of magnesium chloride hexahydrate, this effect on the storage capability

259   of the synthetic sample has been further analyzed.
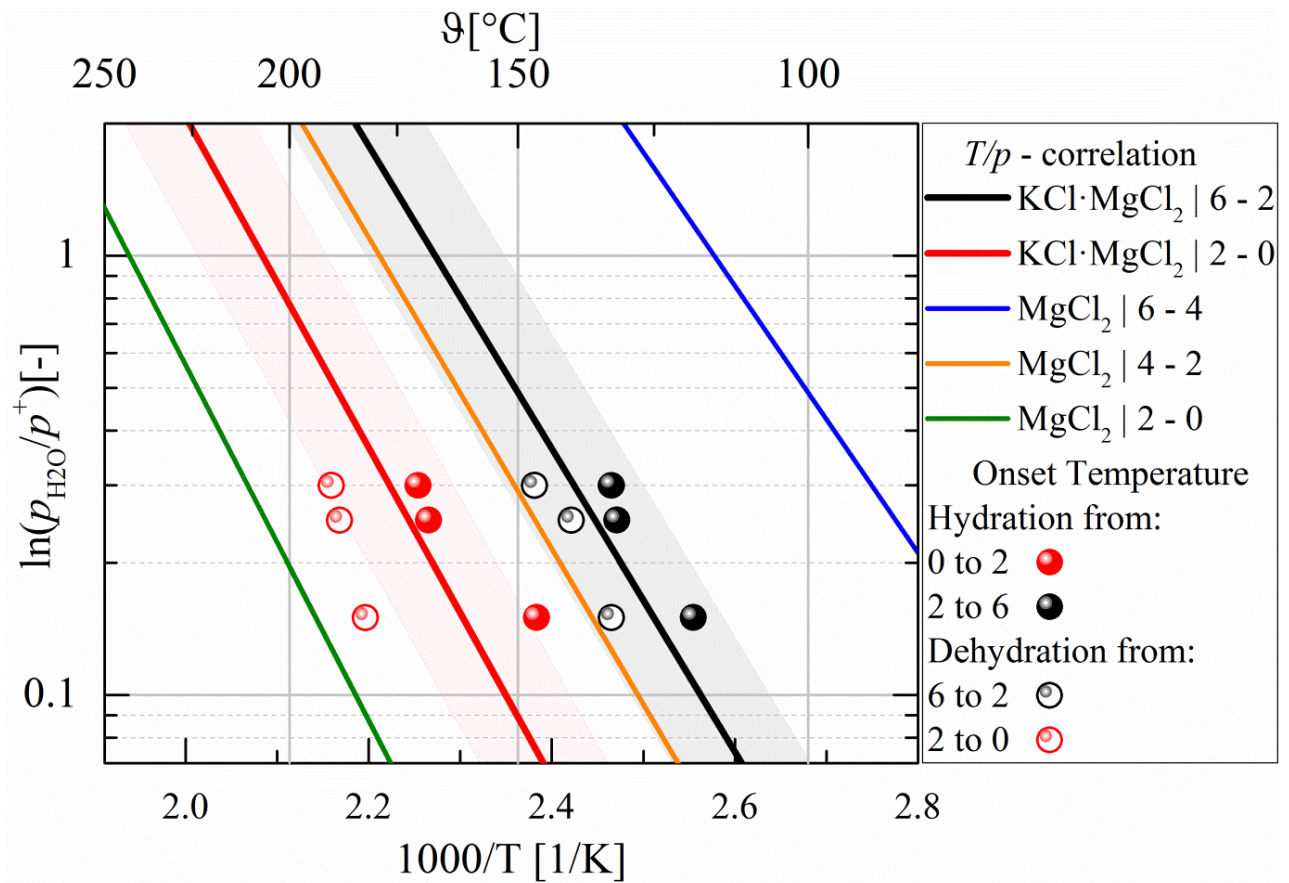
Figure 9 Van't Hoff diagram of carnallite and magnesium chloride hexahydrate. Equilibrium lines calculated for S = 150 J / K mol

Therefore, three more experiments were performed in order to study the cycling stability of the synthetic sample under different operating conditions, based on the steps of reaction showed in Figure 8. These conditions are described in Table 2.

Table 2 Operating conditions of cycle stability experiments performed for 5 cycles

| Experiment | Reaction steps | | Temperature range [°C] | p_{H2O} [kPa] | T/p correlation plotted in Figure 9 |
	Hydration	Dehydration			
2	2	2	100 - 190	25	Black and red lines
3	1	1	140 - 190	25	Red line (2-0)
4	1	1	100 - 150	25	Black line (6-2)

The results of these experiments using the synthetic sample are shown in Figure 10. The mass change during the hydration/dehydration of the sample obtained for the experiment 2 can be

269   seen in Figure 10(a). The first dehydration step (t < 230 min) corresponds to the dehydration

270   of the fresh material that has been performed under dry atmosphere of nitrogen. It can also be

271   seen that the maximum mass increase is lowered for every subsequent cycle. Figure 10 (b)

272   shows the results obtained for the experiment 3 in the Table 2. In this case, the mass increase

273   due to the reversible reaction of hydration over the cycles is lower than in Figure 10 (a),

274   which indicates a faster decomposition of the sample compare to the results of experiment 2.

275   Finally, Figure 10 (c) shows the results obtained from experiment 3 described on Table 2.

276   Results showed a more stable behavior over the cycles, indicating either that there is no

277   decomposition of the sample or that the decomposition is slower under these operating

278   conditions. Additionally, in the results of experiment 4 (Figure 10 (c)) the continuous

279   increase of mass is also observed, in this case in the first two cycles. Since only the

280   temperature conditions were changed, it can be concluded that the temperature level has a

281   direct effect on the cycling stability of the material as well as on the conversion of reaction of

282   the sample.
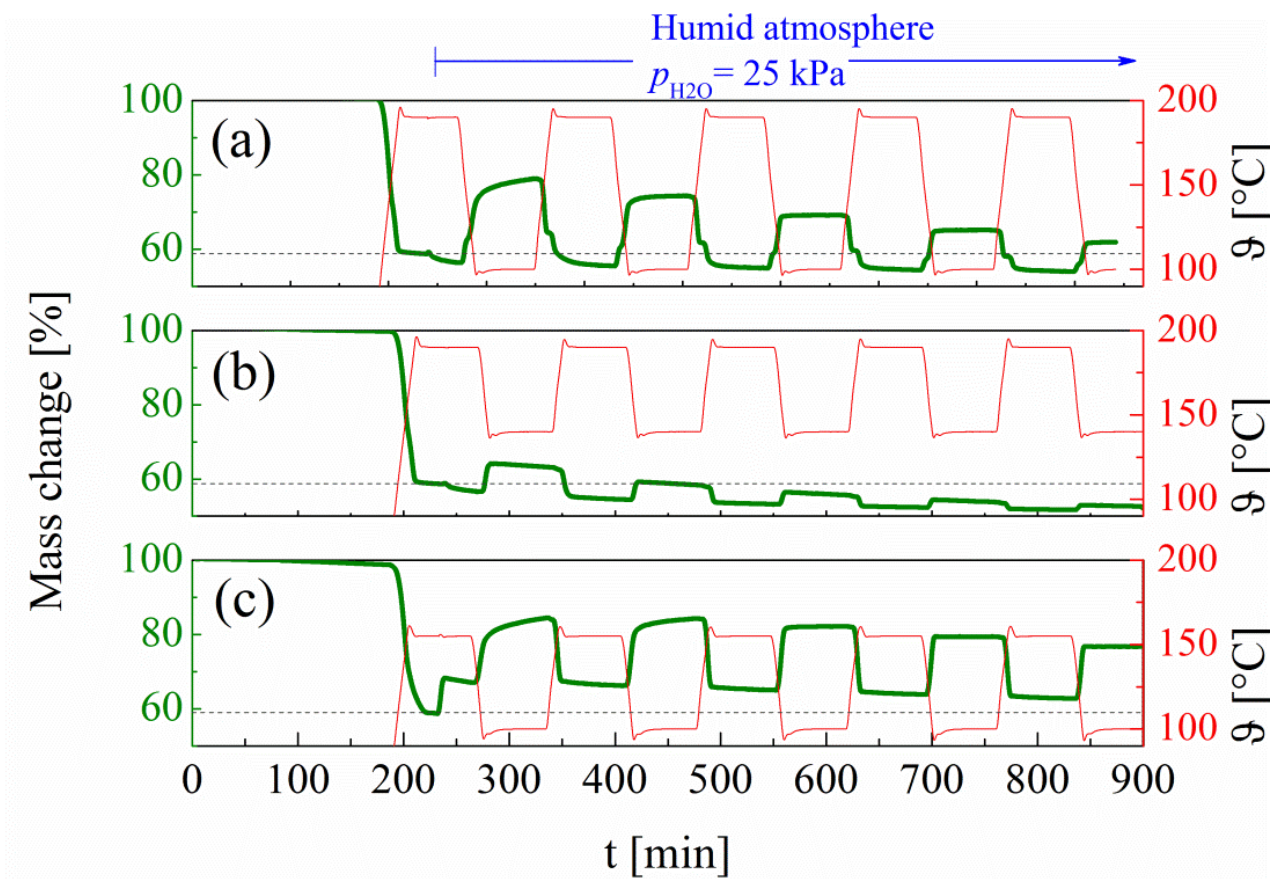
Figure 10 Level of dehydration/hydration of carnallite for five cycles (continuous green curves). (a) Experiment 2, (b) Experiment 3 and (c) Experiment 4

In order to understand the effect of magnesium chloride hexaxydrate on the cyling stability of the synthetic sample, the experiment 2 and experiment 4 were performed using only synthetic magnesium chloride hexahydrate (See Figure S1 and Figure S2 in the supporting information). The results show that this salt is active under these operating conditions. However, after the second cycle the material is completely decomposed (see Figure 11) or is not significantly active anymore (see Figure S3 in the suppoting information).

293
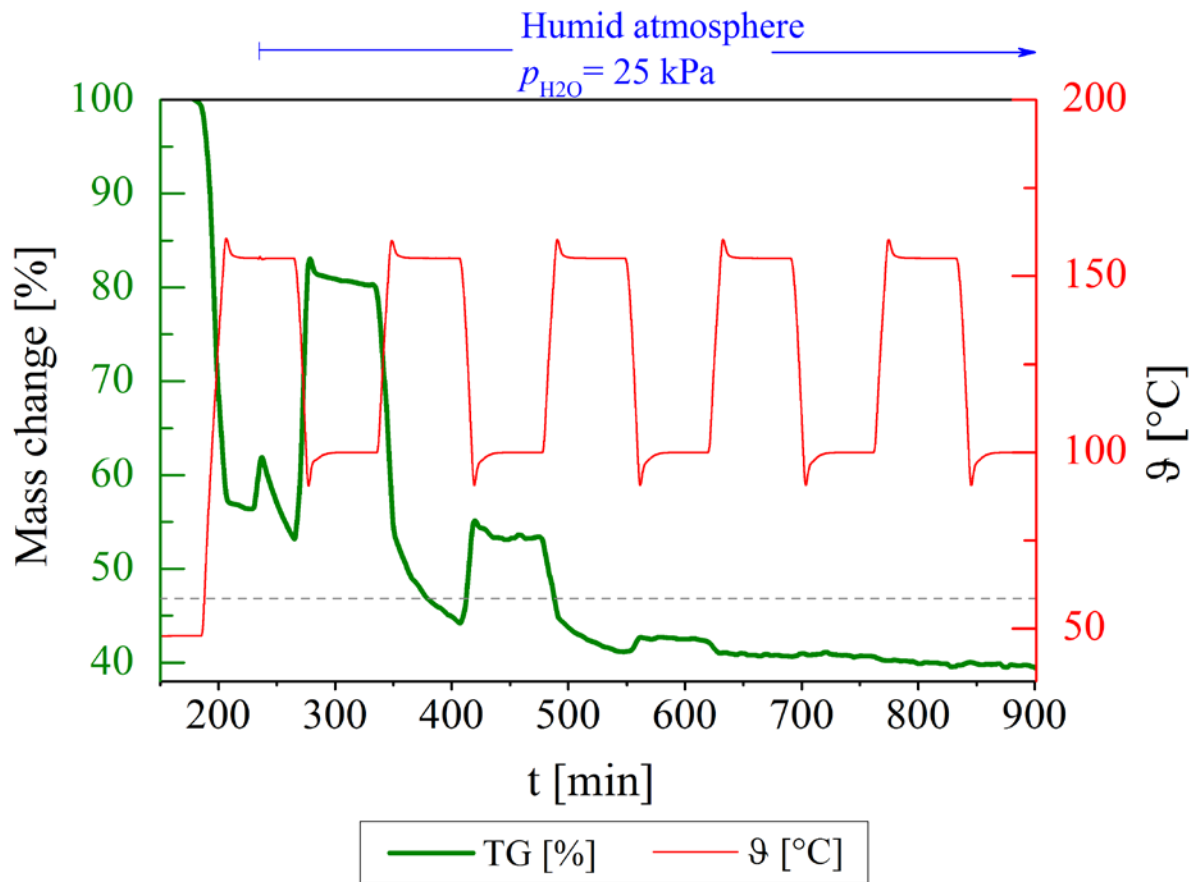
Figure 11 Level of dehydration/hydration of MgCl$_2 \cdot$6H$_2$O for five cycles (Experiment 4); Continuous green curves.

This also explains why the hydration of synthetic sample containing carnallite does not reach equilibrium in the first two cycles, but it does from the third cycle onwards, where magnesium chloride hexahydrate is not active anymore.

In Addition, further investigation on the cycling stability in the long term of the synthetic sample containing carnallite was carried out. To do this, a new experiment (experiment 4.1) was performed. This new experiment was based on experiment 4, but instead of 5 cycles consisted on 15 cycles.The results of experiment 4.1 are shown in Figure 12. In line with the results of experiment 4, the first cycles show the highest increase of mass during the hydration reactions, plus the first two cycles do not reach the equilibrium due to the reaction of magnesium chloride hexahydrate. However, the maximum increase of mass is gradually

306 reduced as the cycles are performed. Furthermore, in every cycle a constant percentage of

307 sample mass is lost (*x wt. %*), corresponding to approximately 1.1 wt. %. This explains the

308 negative slope of the TG-signal base line. In other words, not only do the temperature and the

309 presence of the magnesium chloride hexahydrate influence the conversion of carnallite but

310 they also affect the gradual increase of inactive material, e.g. due to irreversible

311 decomposition caused by hydrolysis. A visualization of this behavior, and the relation

312 between active and inactive material is shown in Figure 13 .
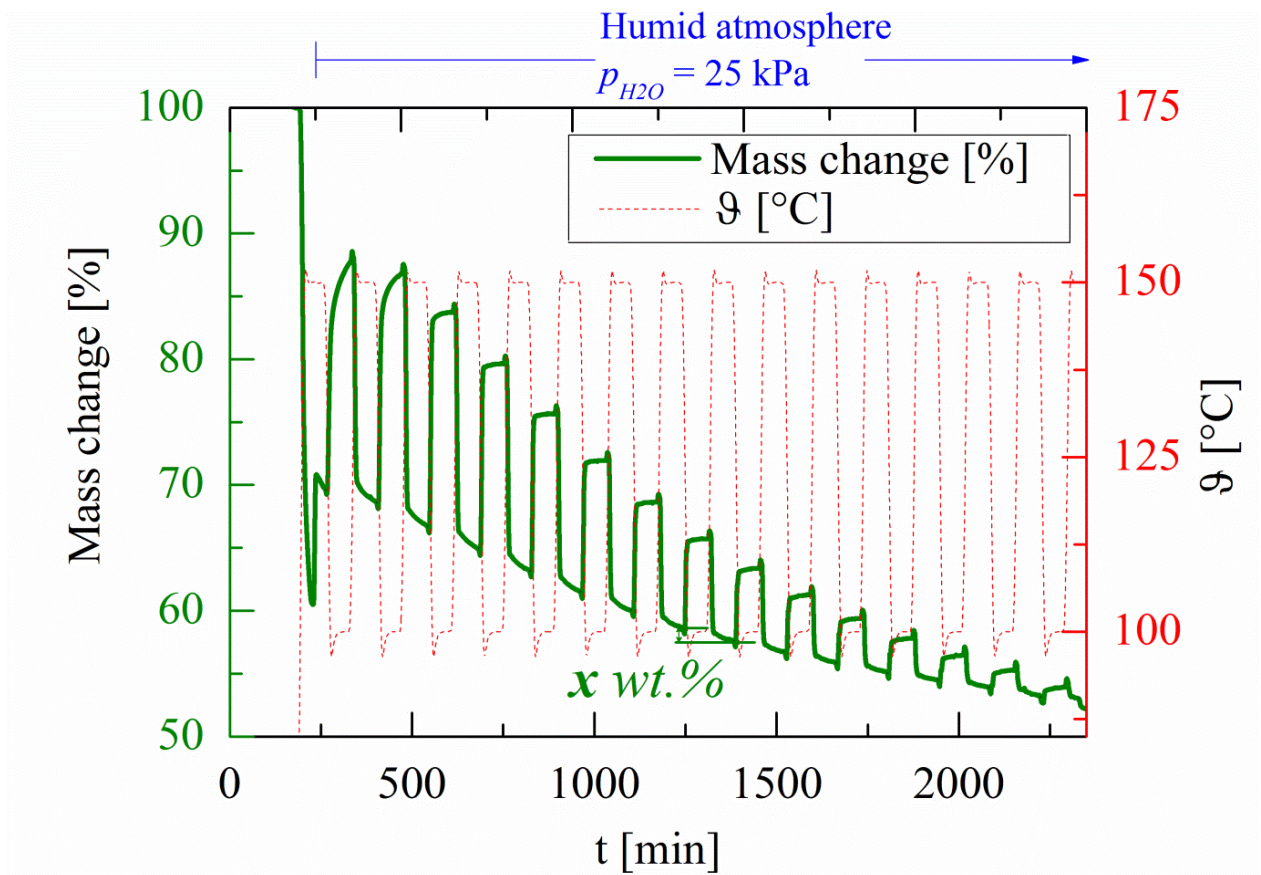
313

314 Figure 12 Measurement of the mass change in the sample of the experiment 4.1
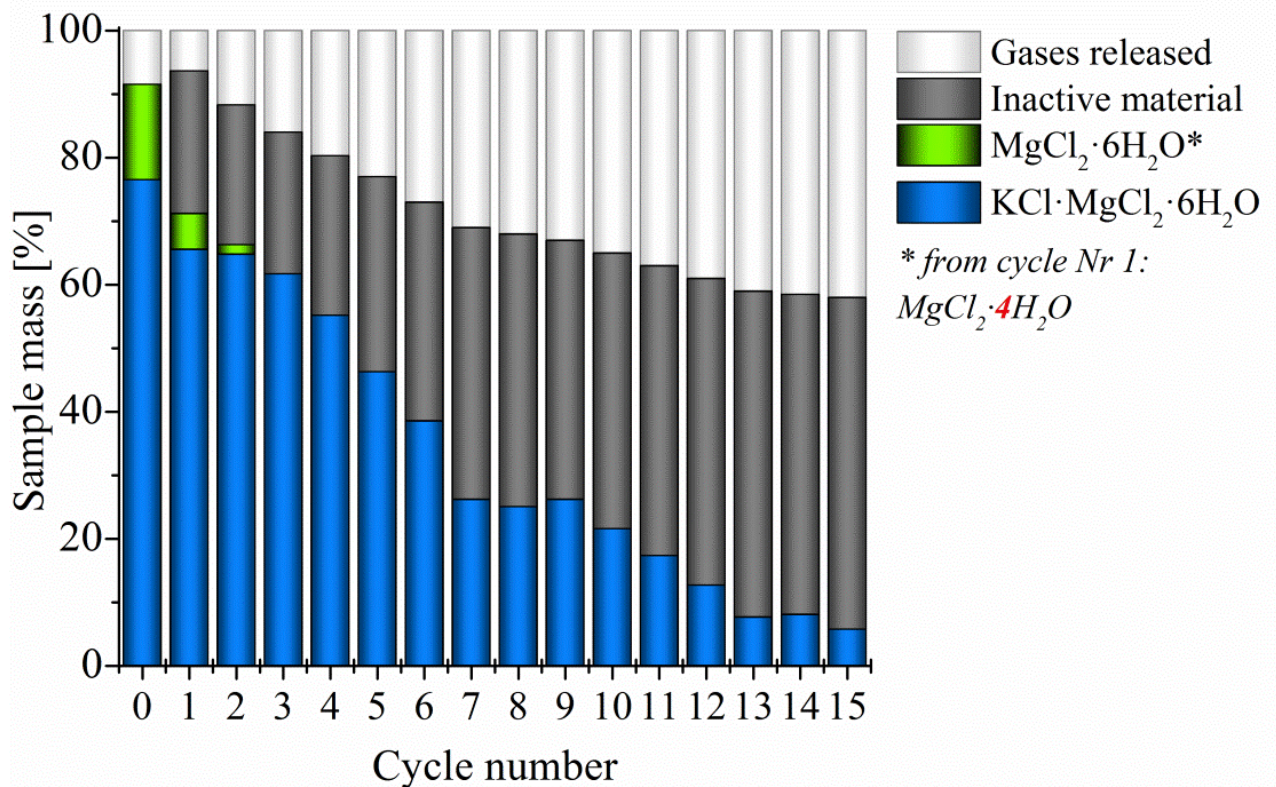
Figure 13 Amount of active and inactive material through cycles based on results from Experiment 4.

These results lead us to the conclusion that after 15 cycles the gradual decomposition of high carnallite-bearing material jeopardizes the feasibility of carnallite for thermochemical storage applications.

One hypothesis for this behavior is related to the presence of molten magnesium chloride hexahydrate or lower hydrates from it. This molten material dissolves or contribute to the decompositions of a small amount of carnallite in every cycle, thus reducing the amount of active material. In addition, this molten material and/or lower hydrates evidence partial hydrolysis which explains the decrease of mass 'x wt. %' with every cycle.

326   Following this hypothesis, factors that could have an influence on the decomposition of

327   magnesium chloride hexahydrate contained in the material were evaluated separately. These

328   are described below:

Influence of crucible material

330   The experiment 4.1 was repeated twice more using different crucible materials, aluminum

331   (Al) crucibles and aluminum oxide (Al_2O_3) crucibles. The results showed that the

332   decomposition of synthetic material, specifically of the magnesium chloride hexahydrate,

333   followed the same path of decomposition already shown in Figure 12 when platinum

334   crucibles were used. That means that the material of the crucible had no influence on the

335   decomposition of magnesium chloride hexahydrate.

Influence of temperature

337   It is possible that the temperature has both a direct and indirect influence on the

338   decomposition of the sample. The indirect influence could be due to the dissociation of

339   carnallite driven by the molten material present in the sample within the operating conditions

340   range. This dissociation could take place either due to the melting process or due to the over

341   hydration of magnesium chloride hexahydrate. This salt hydrate has a melting point of 117

342   °C according to available data and also shows a deliquescent behavior at 22% RH (100

343   °C).[17,25] As a consequence, less carnallite is available, thus the efficiency of reaction is

344   reduced with each cycle. On the other hand, the direct cause could be associated to the

345   hydrolysis reaction of lower hydrates of magnesium chloride hexahydrate ($MgCl_2 \cdot 2H_2O$) Eq.

346   3.[6,23] Although it is extensively reported that this reaction takes place significantly above 180

347   °C, some authors also report that partial hydrolysis of these lower hydrates can take place

348   even from 120 °C.[24,28-30] Additionally, it has been also reported that hydrolysis is more likely

349   to take place in liquid phase compared to the solid phase,[31] behavior that, according to the

350   results obtained in this study, can be also accelerated by the influence of temperature.

$$MgCl_2 \cdot 2H_2O \;\rightarrow\; MgOHCl + HCl_{(g)} + H_2O_{(g)}, \qquad Eq.\,3$$
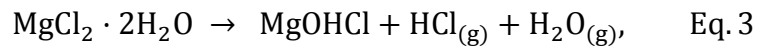
351   In order to investigate if these two factors are responsible of the gradual decomposition of

352   carnallite, the samples resulting from the experiments 2, 3 and 4 (from Figure 10) were

353   analyzed by XRD. The diffractograms are plotted in Figure 14, besides of the diffractogram

354   of fresh synthetic material (black diffractogram), in order to compare the change of the

355   pattern before and after the experiments. The diffractograms of the experiments 2 and 3 (red

356   and blue respectively) show intense peaks that fit with the pattern of potassium chloride. This

357   could confirm that not only the hydrolysis took place during the experiments; since peaks

358   corresponding to magnesium chloride hexahydrate are less intense. But also that carnallite is

359   being gradually dissolved by the molten material, increasing the amount of potassium

360   chloride that is a product of the dissolution of carnallite, and reducing at the same time the

361   amount of 'active material'. In addition, on the diffractograms of experiment 2 and

362   experiment 4, the Korshunovskite ($Mg_2Cl\,(OH)_3 \cdot 4(H_2O)$) was identified. Korshunovskite is

363   comparable to some intermediate products of hydrolysis of magnesium chloride hexahydrate

364   previously reported.[32] Moreover, the product from experiment 3 is the one that showed the

365   highest degree of dissolution of carnallite and decomposition of magnesium chloride

366   hexahydrate, since almost only KCl is identified by XRD.
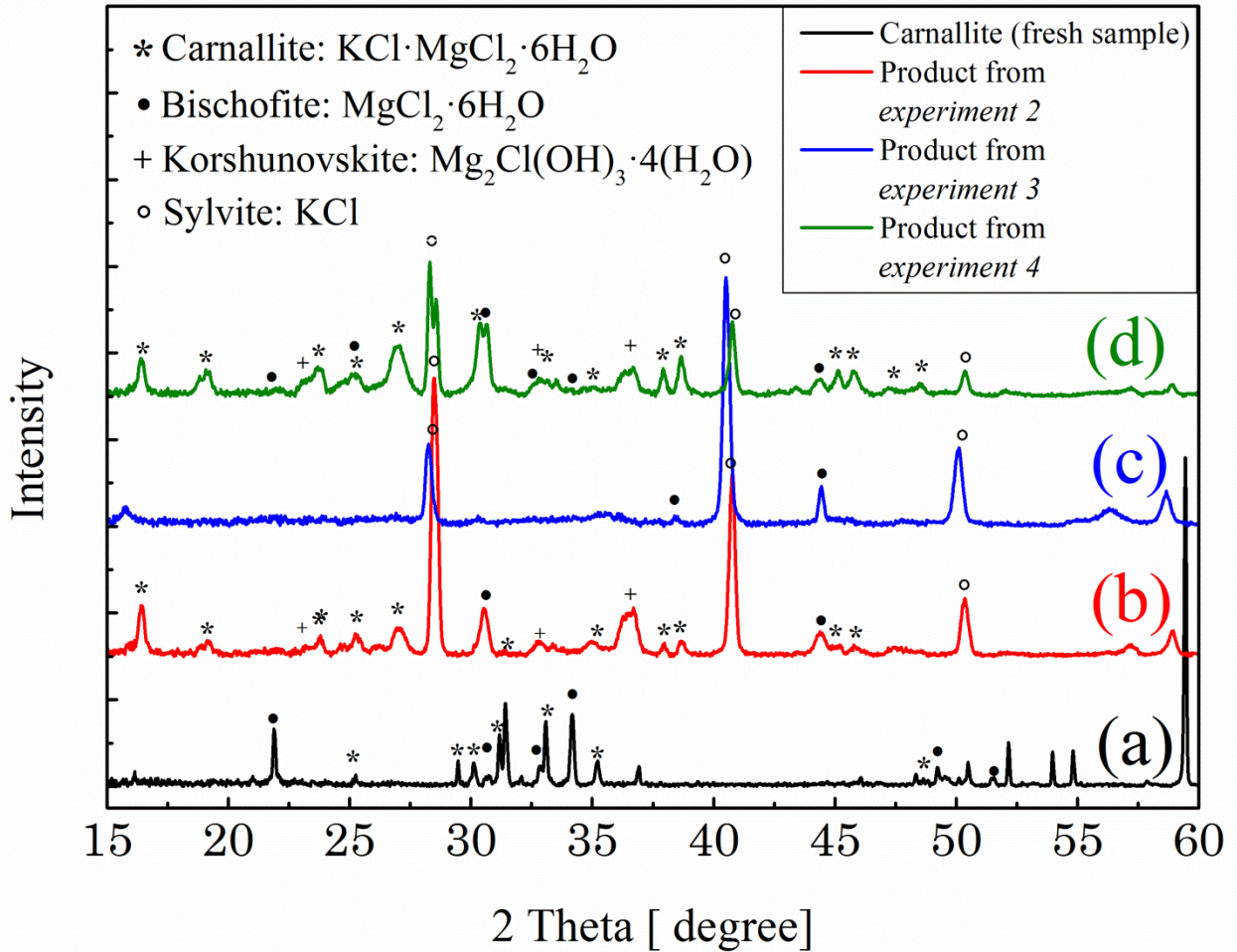
Figure 14 XRD patterns of carnallite (fresh sample) (pattern a) and products after 5 cycle stability experiments 2, 3 and 4), patterns b, c and d, respectively

This indicates that the temperature is the main parameter responsible for accelerating the reduction of active material. Based on this, the 'Experiment 4.1' was repeated reducing the times of isothermal intervals, this experiment was named 'Experiment 4.2'. That means that the experiment 4.2 was performed using intervals of isothermal conditions at 150 °C and 100 °C of 10 min and 20 min, respectively, instead of 60 min.

Results of experiment 4.2 for synthetic material containing carnallite seems to be more stable compared to the behavior during the experiment 4.1, as it is shown in Figure 15. However, in the first 4 cycles, part of the carnallite contained in the synthetic material seems to be inactive. Seeing that less molecules of water are involved in the reactions of hydration and dehydration (~3 mole H_2O).

380   Similarly, a small gradual decomposition can be observed from cycle 8, but the degree of

381   decomposition is significantly smaller and slower. compared to the results of experiment 4.1

382   (Figure 12)This indicates that if the time at which the material is exposed to high

383   temperatures is controlled, the potential to apply carnallite as TCM increases significantly.

384   Also, dehydration (i.e. thermal charging) should be performed at the lowest possible
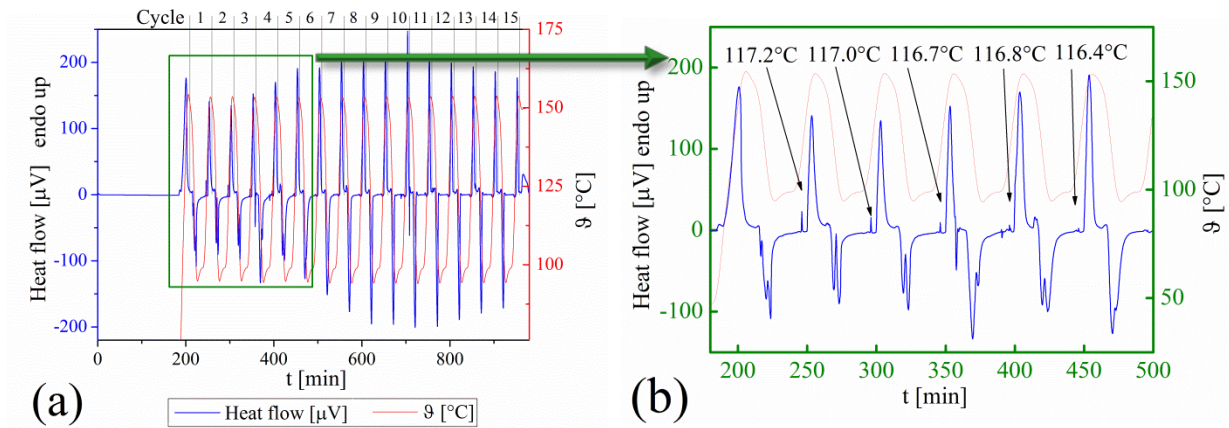
385   temperatures.

386
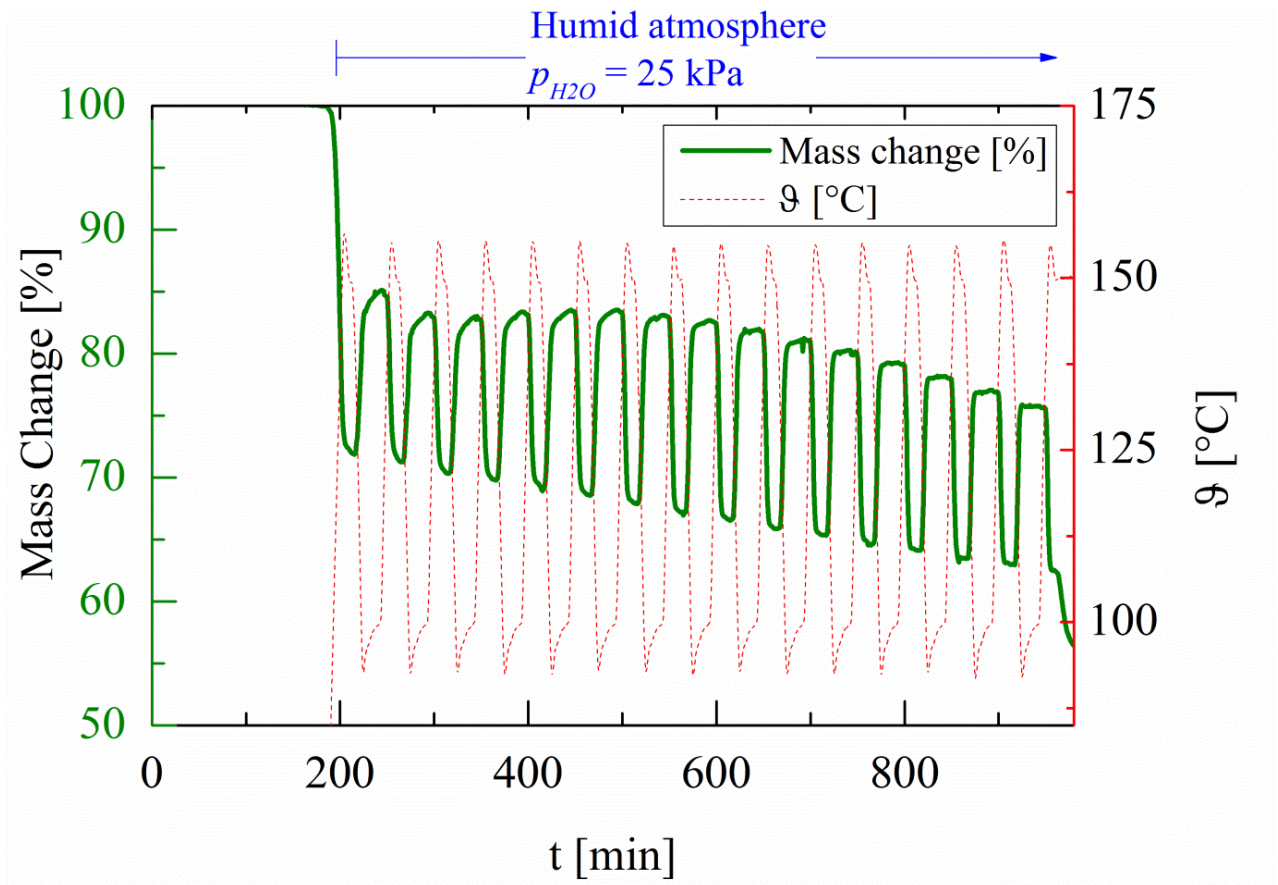
388   Figure 15 Measurement of the mass change in the sample of the experiment 4.2

389   It is still unclear why not all of the reactive material is undergoing a reaction. Nevertheless, it

390   can be influenced by the behavior of $MgCl_2 \cdot 6H_2O$ contained in the sample, which is reacting

391   in the first 6 cycles of this experiment (see Figure 16). This reaction can be identified in the

392 DSC curves of synthetic sample at approximately 117°C. Even though, this temperatures has

393 been extensively reported as the melting point of magnesium chloride hexahydrate by other

394 authors.[2, 4,33- 38]

395 Figure 16 DSC curves obtained from experiment 4.2. Results of the complete experiment (a)
396 and of the first 6 cycles (b).

397 In order to understand if this temperature corresponds to a melting or a chemical reaction

398 under the operating conditions used in this study, the experiment 4.2 was also performed

399 using only synthetic magnesium chloride hexahydrate.

400 The results show that this material is in fact reacting under these operating conditions over

401 the cycles (see Figure 17), on the contrary to the results obtained from experiment 4, where

402 this material was reacting only in the first two cycles. However, based on the molten

403 appareance of the sample at the end of the experiment (See Figure S4 in the supporting

404 information), this reaction is undergoing in liquid phase.

405
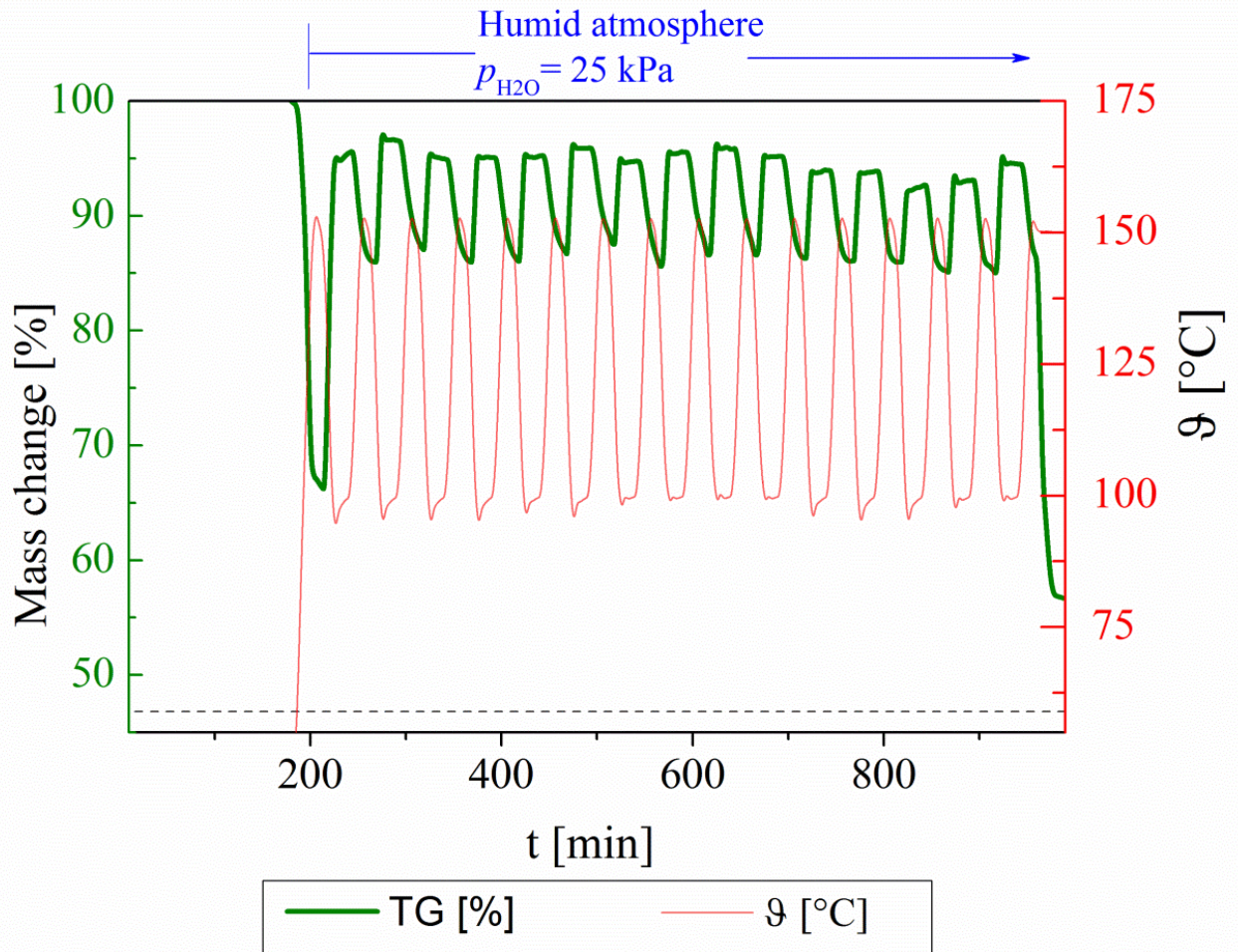
Figure 17 Measurement of the mass change in the synthetic $MgCl_2 \cdot 6H_2O$ of the experiment
4.2

Moreover, the reactions of dehydration and hydration of magnesium chloride hexahydrate are
not complete. In the first cycle, only 3.8 mole of water were released (see Eq. 4) and 3.3 mole
of water reacted during the first hydration step (See Eq. 5). From the second dehydration
onwards, only one mole of water reacts (see Eq. 6)

$$MgCl_2 \cdot 6H_2O \rightarrow MgCl_2 \cdot 2.2H_2O + 3.8H_2O_{(g)} \uparrow \qquad \vartheta_{onset} = 68.5°C \quad (Eq.\,4)$$

$$MgCl_2 \cdot 2.2H_2O + 3.3H_2O_{(g)} \downarrow \rightarrow MgCl_2 \cdot 5.5H_2O \qquad \vartheta_{onset} = 138.1°C \quad (Eq.\,5)$$

$$MgCl_2 \cdot 5.5H_2O \leftrightarrow MgCl_2 \cdot 4.5H_2O + 1H_2O_{(g)} \qquad \vartheta_{onset} = 114.7°C \quad (Eq.\,6)$$
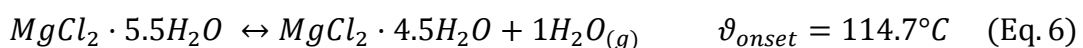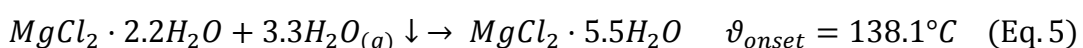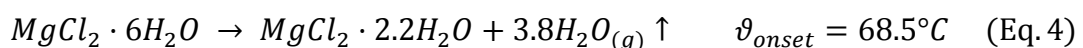
412 Based on results from experiment 4.2 performed for $MgCl_2 \cdot 6H_2O$, could be assumed that the

413 improvement on the behavior showed in Figure 15 is because more $MgCl_2$ is available in the

414 sample, and this is the material that is actually reacting. Nevertheless, the average onset

415 temperatures were obtained from the termogravimetic results as it is shown in Table 3.

416 Furthermore, these temperatures were also added to the van't Hoff diagram as it is shown in

417 Figure 18 The semi transparent bars correspond to the error of each onset temperature. It can

418 be seen that the temperatures at which the reactions start (ϑ_{ONSET}) are different when the

419 experiments were carried out with synthetic sample in comparison with those with "only

420 synthetic $MgCl_2 \cdot 6H_2O$". In the first case, the onset temperatures are significantly close to the

421 $KCl \cdot MgCl_2$ equilibrium temperatures (6-2). While in the second case, the onset temperatures

422 are between the $KCl \cdot MgCl_2$ equilibrium temperatures (6-2) and $MgCl_2$ equilibrium

423 temperautres (6-4).

424 Table 3 Average onset temperatures of synthetic sample and synthetic $MgCl_2 \cdot 6H_2O$ obtained
425 from experiments 4.1 and 4.2

In Figure 18		Experiment 4.1		Experiment 4.2	
		Hydration	Dehydration	Hydration	Dehydration
	Sample	ϑ_{ONSET} (°C)	ϑ_{ONSET} (°C)	ϑ_{ONSET} (°C)	ϑ_{ONSET} (°C)
S_1	Synthetic sample	124.4±7.3	139.9±2.1	129.5±3.0	140.9±1.1
S_2	Only synthetic MgCl2·6H2O	114.0±2.8	114.8±1.1	112.0±2.4	112.5±2.2

426

427
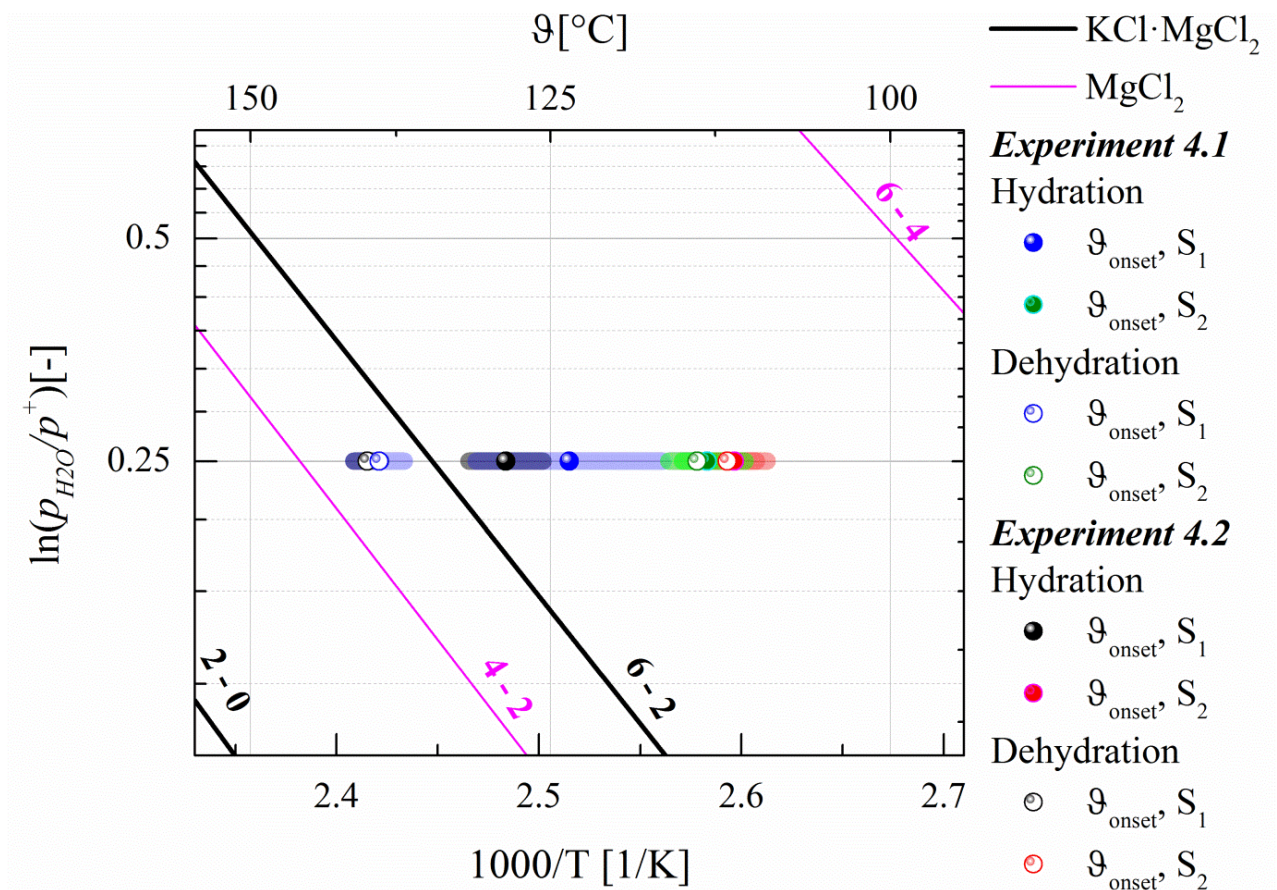
Figure 18 Van't Hoff diagram of KCl·MgCl$_2$·6H$_2$O (carnallite) and MgCl$_2$·6H$_2$O, and their experimental onset temperatures of hydration and dehydration from experiments 4.1 and 4.2.

Under these circumstances it can be conclude that both materials, carnallite and MgCl$_2$·6H$_2$O, are active. However, the mechanism of the effect of MgCl$_2$·6H$_2$O on the reaction of carnallite is yet unclear.

Considering that the reaction of MgCl$_2$·6H$_2$O and carnallite are undergoing simultaneously in the Experiment 4.2,the calculation of active and inactive material in the synthetic sample, was also carried out (see Figure 19). It can be seen that the amount of active material over cycles of this experiment is significantly higher compared to the results obtained from Experiment 4.1, showed in Figure 13.

439
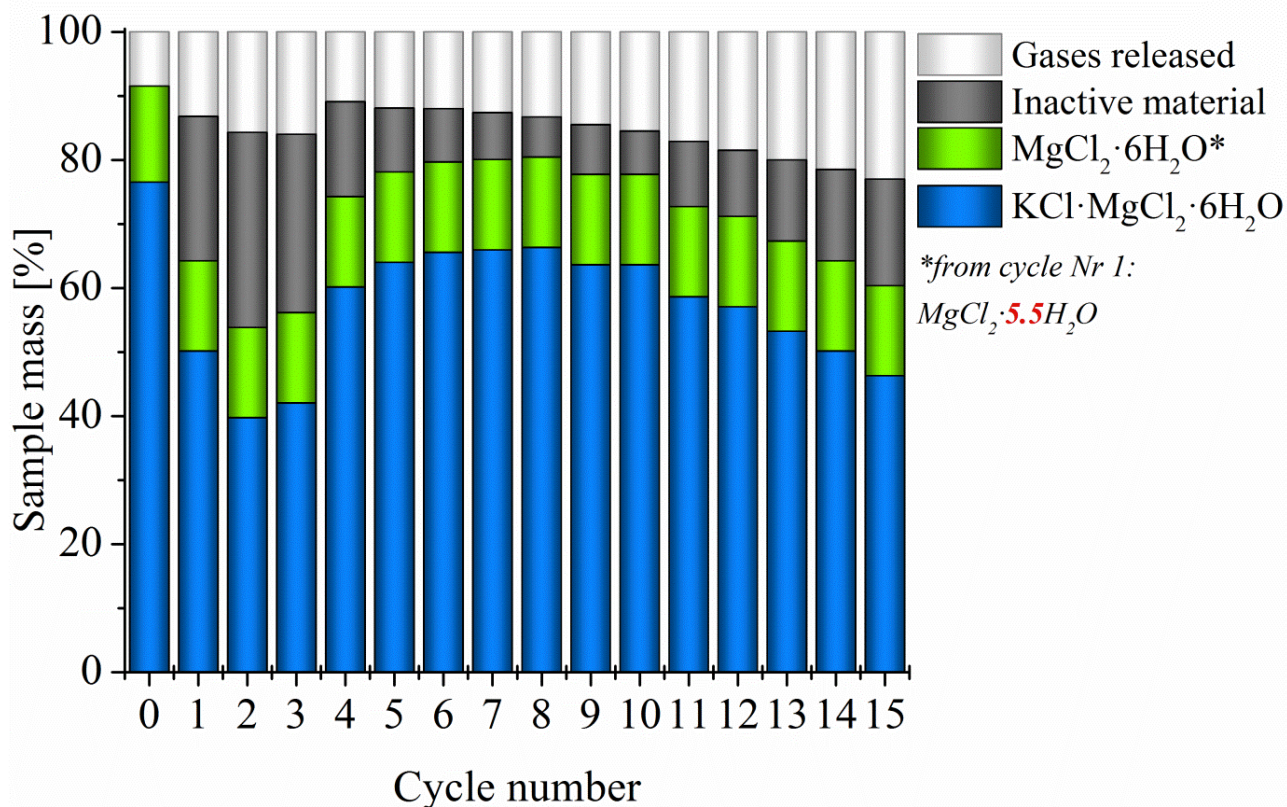
Figure 19 Amount of active and inactive material through cycles based on results of experiment 4.2.

Finally, the effect of temperature and isothermal time on the enthalpies of reaction was analyzed. Figure 20 show the enthalpies of hydration and dehydration obtained from experiments performed for synthetic samples. Figure 20 (a) shows results of experiment 4.1, which, as expected shows a decrease of the enthalpies over cylces, from a maximum absolut value of 168.5 [kJ/mol] to 4.0 [kJ/mol], due to the decomposition of the sample. Results of experiment 4.2 (Figure 20(b)), shows lower yet more constant behavior over cycles with an average absolut value of 99.9 ±13 kJ/mol .
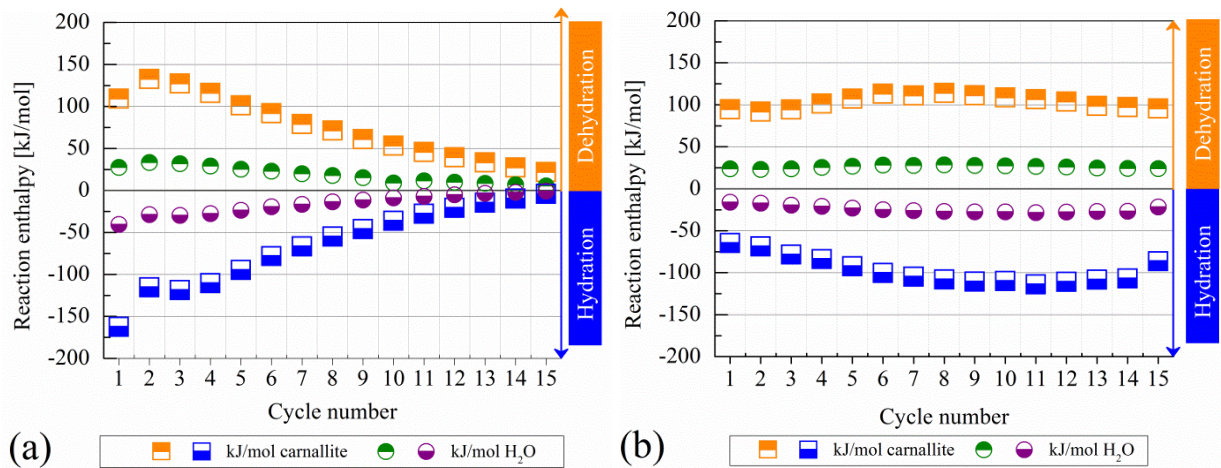
449   Figure 20 Enthalpies of hydration and dehydration from experiment 4.1 and 4.2 for synthetic

450   sample.

451   Using these values, the energy storage density of carnallite was calculated and compared with

452   values reported for other systems of reaction that operate under similar conditions. The

453   results are show in Table 4.

454   Table 4 Enthalpy of reaction and energy storage density for different salt hydrate reaction
455   systems

$MX \cdot nH_2O_{(s)}$	$MX \cdot mH_2O_{(s)}$	(n-m)	$\Delta_R H$ [kJ/mol]	$\Delta_R H/(n-m)$ [kJ/mol]	Price* [Euro/MJ]	esd *** [kWh/m^3]
$KCl \cdot MgCl_2 \cdot 6H_2O$	$KCl \cdot MgCl_2$	6	191.1	31.9	0.05**	303.94
$CaCl_2 \cdot 2H_2O$	$CaCl_2 \cdot 0.3H_2O$	1.7	114.0	67.1	0.21	341.63
$Al_2(SO4)_3 \cdot 18H_2O$	$Al_2(SO4)_3 \cdot 8H_2O$	10	554.5	55.4	0.21	366.57
$LiCl \cdot H2O$	$LiCl$	1	62.2	62.2	11.81	453.64
$LaCl_3 \cdot 7H_2O$	$LaCl_3 \cdot H_2O$	6	355.5	59.3	24.57	421.72
$K_2CO_3 \cdot 1.5H_2O$	K_2CO_3	1.5	95.5	63.7	2.10	254.64

*Considering only the price of medium of storage. Price obtained from Alibaba for industrial quality of materials (www.alibaba.com February 2018).
**The price of low quality bischofite 40US$/ton (31.1 Euro/ton, Freruary 2018), obtained from Salar de Atacama was used as a reference to calculate costs of investment for using carnallite.
*** ρ=1586± 94 [kg/m^3]

456   Following this path, any potential application of this material is definitely limited to low

457   temperature thermal storage or thermal upgrade. Taking the low material cost into account

458   one of the potential applications of this material could also be in the context of long-term heat

459 storage. For this purpose, the temperatures of dehydration can be below 150°C and the

460 temperatures of rehydration close to 40°C under lower water vapor partial pressures (p_{H2O} <

461 1.5 kPa).[26]Additionally, even though this work gives first ideas on how to improve cycling

462 stability of carnallite containing materials as TCM, still further improvements and a better

463 understanding of the decomposition mechanisms are necessary.

464 Apart from the temperature control presented in this study, previous works report different

465 methods in order to prevent the hydrolysis reaction of magnesium salts, during their

466 dehydration. The most popular of all is the dehydration of magnesium chloride hexahydrate

467 or carnallite in atmosphere of HCl in order to increase the amount of $MgCl_2$ for different

468 applications. [28, 31, 39- 41] Due to the hazardousness of HCl, this method has not been tested in

469 this study. Another method suggested is the use of additives in order to improve cycling

470 stability of reaction of magnesium chloride hexahydrate.[42] In case carnallite derived from

471 waste material offers interesting characteristics of a specific application, further studies could

472 evaluate if this method can have the same effect on the investigated material in this study.

473 Future work will concentrate on the investigation of waste material and its comparison with

474 the synthetic one used for this study. Since the amount of carnallite is with around 75%

475 comparable but the presence of bischofite can be excluded, a reduced tendency for hydrolysis

476 can be expected – at least if material impurities contained in the waste material do not have a

477 comparable impact.

478 CONCLUSIONS

479 The thermal stability of a high carnallite-bearing material, its possibility to rehydrate, and

480 consequently its potential operating conditions as a thermochemical energy storage material

481 was identified. That is, the maximum charging temperatures (dehydration) at 150 °C, for 10

482   min, and discharging temperatures (re-hydration) at 100 °C. For both process using 25 kPa of

483   partial vapor pressure in nitrogen.

484   Furthermore, the hydrolysis of magnesium chloride hexahydrate contained in the synthetic

485   material at temperatures below 200 °C was observed. Also the decomposition and/or melting

486   of the magnesium chloride hexahydrate present in the sample was confirmed as an inactive

487   material as well as a low reactive material. This has a strong impact on the cycling stability of

488   carnallite when applied as a thermochemical material. In the first case, because the amount of

489   active material (reactive carnallite) is also reduced under the operating conditions used in this

490   study. As a consequence, the specific capacity of thermochemical storage of carnallite is

491   reduced. And in the second case, even when the reduction of active material was observe, the

492   magnesium chloride hexahydrate seems to have a positive effect on the carnallite, stabilizing

493   it over cycles.

494   Additionally, further experiments to understand the progressive decomposition of carnallite

495   as TCM have been performed. It was shown that the dehydration of carnallite occurs quickly

496   which allows a limit in the time of high temperature exposure. By doing so, a remarkable

497   improvement of the cycling stability of the synthetic material could be observed. However,

498   further improvements on cycling stability are necessary if carnallite should be used in

499   thermochemical storages.

500   ASSOCIATED CONTENT

501   Supporting information

502   The operating conditions of Experiment 2 and experiment 4 using $MgCl_2 \cdot 6H_2O$, the van't

503   Hoff plot of $KCl \cdot MgCl_2$ and $MgCl_2$ with the respective operating conditions of both

504 experiments, results of Experiment 2 using $MgCl_2 \cdot 6H_2O$ and molten sample after experiment

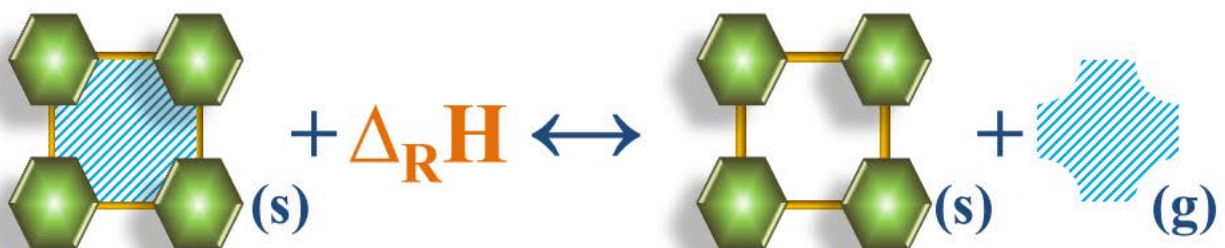505 4.2.

506 AUTHOR INFORMATION

507 Corresponding author

508 *E-mail: andrea.gutierrezrojas@dlr.de
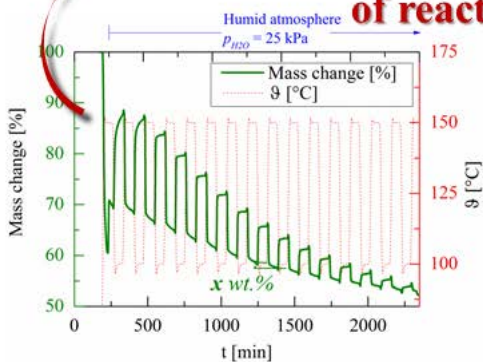
509 *Tel: +49-(0)711-6862-8236

510 ACKNOWLEDGEMENTS

515 TOC/ABSTRACT GRAPHIC
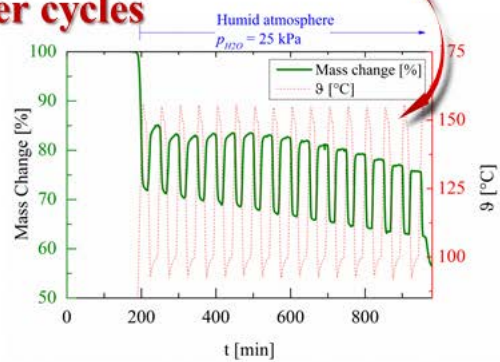
516

517 SYNOPSIS: Once identified the critical operational limits for carnallite the control of

518 temperature improves the cycling stability of chemical reactions (heat storage).

519 REFERENCES

520 1. Hasnain, S. M. review on sustainable thermal energy storage technologies, part I: Heat

521   storage materials and techniques. *Energy Convers. Mgmt.* **1998**, 39 (11),1127 – 1138,

522   DOI 10.1016/S0196-8904(98)00025-9.

523 2. Sharma, A.; Tyagi, V.V.; Chen, C.R.; Buddhi, D. Review on thermal energy storage with

524   phase change materials and applications, *Renew. Sustainable Energy Rev.* **2009**, 13 (2),

525   318 – 345, DOI 10.1016/j.rser.2007.10.005.

526 3. Miró, L.; Navarro, M. E.; Suresh, P.; Gil, A.; Fernandez, A. I.; Cabeza, L. F.

527   Experimental characterization of a solid industrial by-product as material for high

528   temperature sensible thermal energy storage (TES). *Appl. Energy.* **2014**, 113, 1261 –

529   1268, DOI 10.1016/j.apenergy.2013.08.082.

530 4. Ushak, S.; Gutierrez, A.; Galleguillos, H.; Fernandez, A. G.; Cabeza, L. F.; Grágeda, M.

531   Thermophysical characterization of a by-product from the non-metallic industry as

532   inorganic PCM, *Sol. Energy Mater Sol. Cells.* **2015**, 132, 385 – 391, DOI

533   10.1016/j.solmat.2014.08.042.

534 5. Gutierrez, A.; Miró, L.; Gil, A.; Rodríguez-Aseguinolaza, J.; Barreneche, C.; Calvet, N.;

535   Py, X.; Fernández, A. I.; Grágeda, M.; Ushak, S.; Cabeza, L.F. Advances in the

536   valorization of waste and by-product materials as thermal energy storage (TES)

537   materials, *Renew. Sustainable Energy Rev.* **2016**, 59, 763–783, DOI

538   10.1016/j.rser.2015.12.071.

539 6. Gutierrez, A.; Ushak, S.; Mamani, V.; Vargas, P.; Barreneche, P.; Cabeza, L. F.;

540   Grágeda, M.; Characterization of wastes based on inorganic double salt hydrates as

541   potential thermal energy storage materials, *Sol. Energy Mater Sol. Cells.* **2017**, 170, 149–

542   159, DOI 10.1016/j.solmat.2017.05.036.

543 7. Letcher, T. M., *In Storing Energy: with Special Reference to Renewable Energy Sources*,

544   1st ed.; Press: Elsevier, Oxford, 2016.

545 8. Hadorn, J. C. Advanced storage concepts for active solar energy. In proceedings of:

546   EUROSUN 2008 1st International congress on heating, cooling and Buildings, October

547   7th to 10th, Lisbon – Portugal.

548 9. Abedin, A. H; Rosen, M. A. A critical review of thermochemical energy storage systems.

549   *The open renewable energy storage journal*, **211**, 4, 42 – 46, DOI

550   10.2174/1876387101004010042.

551 10. Weck, P.F.; Kim, E.; Solar energy storage in phase change materials: First-Principles

552   thermodynamic modeling of magnesium chloride hydrates, *J. Phys. Chem. C*, **2014**, 118

553   (9), 4618 – 4625, DOI 10.1021/jp411461m.

554 11. Lizana, J.; Chacartegui, R.; Barrios-Padura, A.; Valverde, J. M.; Advances in thermal

555   energy storage materials and their applications towards zero energy buildings: A critical

556   review. *Appl. Energy*. **2017**, 203, 219-239, DOI 10.1016/j.apenergy.2017.06.008.

557 12. Solé, A., Fontanet, X., Barreneche, C.; Fernández, A.I.; Martorell, I.; Cabeza, L. F.

558   Requirements to consider when choosing a thermochemical material for solar energy

559   storage, *Sol. Energy*. **2013**, 97, 398–404, DOI 10.1016/j.solener.2013.08.038.

560 13. Richter, M.; Bouché, M.; Linder, M.; Heat transformation based on CaCl2/H2O – Part

561   A: Closed operation principle, *Appl. Therm. Eng*. **2016**, 102, 615-621, DOI

562   10.1016/j.applthermaleng.2016.03.076.

563 14. Bouché, M.; Richter, M.; Linder, M.; Heat transformation based on CaCl2/H2O – Part B:

564   Open operation principle, *Appl. Therm. Eng*, **2016**, 102, 641-647, DOI

565   10.1016/j.applthermaleng.2016.03.102.

566   15. Richter, M.; Habermann, E.M.; Siebecke, L.; Linder, M. A systematic screening of salt

567   hydrates as materials for a thermochemical heat transformer. *Thermochim. Acta.* **2018**,

568   659, 136 – 150, DOI 10.1016/j.tca.2017.06.011

569   16. Cabeza, L.F. ed. *Advances in thermal energy storage systems: Methods and applications.*

570   1st ed.Press: Elsevier. **2014**.

571   17. Donkers, P. A. J. Experimental study on thermochemical heat storage materials. Ph.D.

572   Dissertation, Eindhoven University of Technology, Eindhoven, Netherlands, 2015.

573   18. Mamani, V., Gutierrez, A., Li21nder, M., Ushak, S. Characterization of an industrial

574   waste based on double salt hydrate with potential use as thermochemical material. In

575   proceedings: SDEWES - 1st Latin American conference on sustainable development of

576   energy, water and environment systems, 2018, January 28th to 31th, Rio de Janeiro –

577   Brazil.

578   19. Mamani, V., Gutierrez, A., Ushak, A., . Inorganic Industrial Wastes used as

579   Thermochemical Energy Storage Materials. In: Proceedings of SWC 2017 / SHC 2017

580   2017 October 29- November 02, Abu Dhabi, United Arab Emirates; 2017

581   20. Korotkov, J.A.; Mikhkailov, E. F.; Andreevm, G. A.; Eltsov, B. I.; Plyakov, J.A.;

582   Shestakov, B. G.; Kechina, G. D. Method of dehydrating carnallite. *United States Patent.*

583   Patent Nr. 4,224,291. **1980**

584   21. Molenda, M.; Stengler, J.; Linder, M.; Wörner, A. Reversible hydration behavior of

585        $CaCl_2$ at high H_2O partial pressures for thermochemical energy storage. *Thermochim.*

586   *Acta*. **2013**, 560, 76 – 81, DOI 10.1016/j.tca.2013.03.020.

587   22. Emons, H.-H.; Naumann, R.; Pohl, T.; Voigt, H. Thermoanalytical investigations on the

588   decomposition of double salts: I. the decomposition of carnallite. *J. Therm. Anal.*

589   *Calorim*. **1984**, 29 (3), 571-579, DOI 10.1007/BF01913466.

590   23. Friedrich, H. E.; Mordike, B.L. *Magnesium Technology, Metallurgy, Design Data,*

591   *Applications*.1st ed.; Press: Springer, Berlin Heidelberg, **2006**.

592   24. Zondag, H.A.; van Essen, V.M.; Bleijendaal, L.P.J.; Kikkert, B.W.J.; Bakker, M.

593   Application of $MgCl_2 \cdot 6H_2O$ for thermochemical seasonal solar heat storage. Presented at

594   the the 5th International Renewable Energy Storage Conference IRES 2010. Berlin,

595   Germany. **2010**

596   25. Ferchaud, C.J.; Zondag, H.A.; Veldhuis, J.B.; de Boer, R. Study of the reversible water

597   vapour sorption process of $MgSO_4$ $7H_2O$ and $MgCl_2 6H_2O$ under the conditions of

598   seasonal solar heat storage. *J. Phys.: Conf. Ser*. **2012**, 395, 012069, DOI 10.1088/1742-

599   6596/395/1/012069.

600   26. Gutierrez, A.; Ushak, S.; Linder, M. Carnallite as potential thermochemical energy

601   storage material for seasonal heat storage applications. In proceedings: IWLiME 2017 -

602   4th International Workshop on Lithium, Industrial Minerals and Energy, 2017,

603   September 25th – 27th, Cochabamba – Bolivia.

604   27. Donkers, P.A.J.; Sögütoglu, L.C.; Huinink, H.P.; Fischer, H.R.; Adan, O.C.G. A review

605   of salt hydrates for seasonal heat storage in domestic applications. *Appl.* Energy. **2017**,

606   199, 45–68, DOI 10.1016/j.apenergy.2017.04.080.

607   28. Kelley, K. K. Energy requeriments and equilibria in the dehydration, hydrolysis, and

608   decomposition of magnesium chloride. United States government printing office

609   Washington. **1945**.

610   29. Mamani, V.; Gutierrez, A.; Ushak, S. Development of low-cost inorganic salt hydrate as

611   a thermochemical energy storage material. *Sol. Energy Mater Sol. Cells*. **2017**, 176, 346-

612   356, DOI 10.1016/j.solmat.2017.10.021.

613   30. Ferchaud, C. Experimental study of salt hydrates for thermochemical seasonal heat

614   storage. Ph.D. Dissertation, Eindhoven University of Technology, Eindhoven,

615   Netherlands, **2016**.

616   31. Smeets, B.; Iype, E.; Nedea, S. V.; Zondag, H. A.; Rindt, C. C. M. A DFT based

617   equilibrium study on the hydrolysis and the dehydration reactions of $MgCl_2$ hydrates. *J*

618   *Chem Phys*. **2013**, 139, 12, 124312, DOI 10.1063/1.4822001.

619   32. Huang, Q.; Lu, G.; Wang, J.; Yu, J. Thermal decomposition mechanisms of $MgCl_2 \cdot 6H_2O$

620   and $MgCl_2 \cdot H_2O$. *J. Anal. Appl. Pyrolysis*. **2011**, 91 (1), 159–164, DOI

621   10.1016/j.jaap.2011.02.005.

622   33. Zalba, B., Marín, J.M., Cabeza, L.F., Mehling, H. Review on thermal energy storage

623   with phase change: materials, heat transfer analysis and applications, *Appl. Therm. Eng.*

624   **2003**, 23 (3), 251–283, DOI 10.1016/S1359-4311(02)00192-8.

625   34. Cabeza, L. F., Castell, A., Barreneche, C., de Gracia, A., Fernández, A. I. Materials used

626   as PCM in thermal energy storage in buildings: a review. *Renew. Sustainable Energy Re.*

627   **2011**, 15 (3), 1675-1695, DOI 10.1016/j.rser.2010.11.018.

628   35. Abhat, A. Low temperature latent heat thermal energy storage: heat storage materials,

629   *Sol. Energy*, **1983**, 30 (4), 313-332, DOI 10.1016/0038-092X(83)90186-X.

630   36. Dincer, I., Rosen, M.A. Thermal energy storage, systems and applications, 2nd ed.; John

631   Wiley & Sons, Ltd, Press: Chichester, 2002.

632   37. Naumann, R., Emons, H.H. Results of thermal analysis for investigation of salt hydrates

633   as latent heat-storage materials, *J. Therm.Anal*. **1989**, 35 (3), 1009-1031, DOI

634   10.1007/BF02057256.

635   38. Mehling, H., Cabeza, L.F. Heat and cold storage with PCM. An up to Date introduction

636   into basics and applications, 1st Ed.; Springer Press: Berlin Heidelberg, 2008.

637   39. Kipouros, G. J.; Sadoway, D. R. A thermochemical analysis of the production of

638   anhydrous $MgCl_2$. *J. Light Met*. **2001**,1 (2), 111-117, DOI 10.1016/S1471-

639   5317(01)00004-9.

640   40. Moscowitz, H.; Lando, D.; Cohen, H.; Wolf, D. Bishophite Chlorination, *Ind. Eng.*

641   *Chem. Prod. Res. Dev*. **1978**, 17 (2), 156–160, DOI 10.1021/i360066a013.

642   41. Liu, X.; Cui, X. Research progress in dehydration technology of bischofite for preparing

643   anhydrous magnesium chloride. 5th International Conference on Civil, Architectural and

644   Hydraulic Engineering (ICCAHE 2016). **2016**, 261-267.

645   42. Rammelberg, H. U.; Osterland, T.; Priehs, B.; Opel, O.; Ruck, W. K. L. Thermochemical

646   heat storage materials – Performance of mixed salt hydrates. *Sol. Energy*. **2016**, 136,

647   571–589, DOI 10.1016/j.solener.2016.07.016.